

Award Number: WQ81XWH-11-2-0021

TITLE: "Threshold-Switchable Particles (TSP) to Control Internal Hemorrhage"

PRINCIPAL INVESTIGATOR: James H. Morrissey, Ph.D.

CONTRACTING ORGANIZATION: University of Illinois, Urbana, IL 61801-3620

REPORT DATE: December 2013

TYPE OF REPORT: Annual

PREPARED FOR: U.S. Army Medical Research and Materiel Command  
Fort Detrick, Maryland 21702-5012

DISTRIBUTION STATEMENT: Approved for Public Release;  
Distribution Unlimited

The views, opinions and/or findings contained in this report are those of the author(s) and should not be construed as an official Department of the Army position, policy or decision unless so designated by other documentation.

<b>REPORT DOCUMENTATION PAGE</b>				<i>Form Approved</i> <b>OMB No. 0704-0188</b>	
Public reporting burden for this collection of information is estimated to average 1 hour per response, including the time for reviewing instructions, searching existing data sources, gathering and maintaining the data needed, and completing and reviewing this collection of information. Send comments regarding this burden estimate or any other aspect of this collection of information, including suggestions for reducing this burden to Department of Defense, Washington Headquarters Services, Directorate for Information Operations and Reports (0704-0188), 1215 Jefferson Davis Highway, Suite 1204, Arlington, VA 22202-4302. Respondents should be aware that notwithstanding any other provision of law, no person shall be subject to any penalty for failing to comply with a collection of information if it does not display a currently valid OMB control number. <b>PLEASE DO NOT RETURN YOUR FORM TO THE ABOVE ADDRESS.</b>					
<b>1. REPORT DATE</b> December-2013		<b>2. REPORT TYPE</b> Annual		<b>3. DATES COVERED</b> 23 November 2012 –22 November 2013	
<b>4. TITLE AND SUBTITLE</b>  "Threshold-Switchable Particles (TSP) to Control Internal Hemorrhage"				<b>5a. CONTRACT NUMBER</b> W81XWH-11-2-0021	
				<b>5b. GRANT NUMBER</b> W81XWH-11-2-0021	
				<b>5c. PROGRAM ELEMENT NUMBER</b>	
<b>6. AUTHOR(S)</b> James H. Morrissey, Rustem Ismagilov, Ying Liu, and Galen Stucky				<b>5d. PROJECT NUMBER</b>	
				<b>5e. TASK NUMBER</b>	
				<b>5f. WORK UNIT NUMBER</b>	
<b>7. PERFORMING ORGANIZATION NAME(S) AND ADDRESS(ES)</b> UNIVERSITY OF ILLINOIS GRANTS AND CONTRACTS OFFICE 506 SWRIGHT ST, 364 HENRY ADMIN BLDG URBANA IL 61801-3620				<b>8. PERFORMING ORGANIZATION REPORT NUMBER</b>	
<b>9. SPONSORING / MONITORING AGENCY NAME(S) AND ADDRESS(ES)</b> U.S. Army Medical Research and Materiel Command Fort Detrick, Maryland 21702-5012				<b>10. SPONSOR/MONITOR'S ACRONYM(S)</b>	
				<b>11. SPONSOR/MONITOR'S REPORT NUMBER(S)</b>	
<b>12. DISTRIBUTION / AVAILABILITY STATEMENT</b> Approved for Public Release; Distribution Unlimited					
<b>13. SUPPLEMENTARY NOTES</b>					
<b>14. ABSTRACT</b>  The final goal of this project is to develop smart particles to stop internal hemorrhage at local sites. Four collaborating laboratories are working together under this contract to define threshold levels of activators of blood clotting such that the candidate clotting activators will circulate in the blood at a concentration below the threshold necessary to trigger clotting, but accumulation of the activators at sites of internal injury/bleeding will cause the local concentration of clotting activators to exceed the clotting threshold and restore hemostasis. During the past year we have applied our improved methods for covalently attaching inorganic polyphosphate (a potent initiator and accelerator of blood clotting) to nanoscale solid supports including silica- and gold-based nanoparticles that have been fabricated using a variety of derivitization and passivation methods. We have conducted extensive testing of candidate procoagulant nanoparticles to quantify their ability to trigger and/or accelerate blood clotting and have made significant progress toward the goal of adjustable procoagulant activities of the particles to render them sub- or supra-threshold with regard to initiation of the clotting cascade.					
<b>15. SUBJECT TERMS</b> Internal hemorrhage; Bleeding; Blood clotting; Nanoparticles; Trauma					
<b>16. SECURITY CLASSIFICATION OF:</b>			<b>17. LIMITATION OF ABSTRACT</b>  UU	<b>18. NUMBER OF PAGES</b>  35	<b>19a. NAME OF RESPONSIBLE PERSON</b> USAMRMC
<b>a. REPORT</b> U	<b>b. ABSTRACT</b> U	<b>c. THIS PAGE</b> U			<b>19b. TELEPHONE NUMBER</b> (include area code)

## Table of Contents

	<u>Page</u>
Introduction.....	1
Body.....	1
Key Research Accomplishments.....	29
Reportable Outcomes.....	30
Conclusion.....	31
References.....	32
Appendices .....	(none)

# **THIRD ANNUAL REPORT: WQ81XWH-11-2-0021: "Threshold-Switchable Particles (TSP) to Control Internal Hemorrhage"**

## **INTRODUCTION**

The final goal of our research is to develop smart particles to stop internal hemorrhage at local sites. In working toward this goal, we combine multiple approaches in four collaborating laboratories to define threshold levels of activators of blood clotting such that the candidate clotting activators will circulate in the blood at a concentration below the threshold necessary to trigger clotting. On the other hand, when the particles accumulate at sites of internal injury/bleeding, their local concentration should exceed the clotting threshold and restore hemostasis. Our continuing approaches include the development and application of chemistries for attaching inorganic polyphosphate (polyP; a potent trigger and accelerator of blood clotting) to nanoscale solid supports, development of candidate nanoparticles with varying abilities to trigger and/or accelerate blood clotting, and defining the threshold levels under which these particles will or will not trigger blood clotting.

## **BODY**

### **Comments on Administrative and Logistical Matters**

**Subcontracts** — Four laboratories participate in this project, headed by Drs. James Morrissey (University of Illinois at Urbana-Champaign), Ying Liu (University of Illinois at Chicago), Rustem Ismagilov (originally at the University of Chicago; now at Caltech), and Galen Stucky (University of California at Santa Barbara). The primary contract was awarded to the University of Illinois, with Dr. Morrissey as the PI. The Morrissey and Liu laboratories are at University of Illinois campuses (Urbana-Champaign and Chicago), so subaward contracts were not needed and grant accounts were set up for both investigators during the first quarter. The laboratories of Drs. Ismagilov and Stucky are located at other universities, which required negotiating subcontracts to both of these sites. The subaward agreement to the University of Chicago (Ismagilov lab) was completed in February 2011, and the subaward agreement with the University of California at Santa Barbara (Stucky lab) was completed in March 2011. Dr. Ismagilov moved his laboratory to Caltech in October 2011, and a new subaward contract to Caltech was finalized at the end of May 2012 in order for Dr. Ismagilov to continue his studies funded in this project. Thus, the move of the Ismagilov laboratory to Caltech resulted in a hiatus in funding to the Ismagilov lab from October 2011 through May 2012, which has slowed overall progress on this project. As detailed in the next paragraph, we anticipate adding a new subaward to Dr. Christian Kastrup, who will take on a certain of the planned studies in a close collaboration with Dr. Ismagilov.

**No-cost extension** — Given the delays in the project as a consequence of the relocation of the Ismagilov lab to Caltech, progress on certain of the subtasks of this proposal has been delayed. We therefore request a one-year, no-cost extension of this proposal, which was recently granted, resulting in a new expiration date of June 22, 2014. The Stucky, Liu and Morrissey labs have continued to make progress in the designing, making and testing a variety of procoagulant nanoparticles as candidate Threshold-Switchable Particles (TSPs). As noted above, the move of the Ismagilov lab and the difficulties in re-starting his portion of the project delayed the detailed microfluidics-based testing of our TSP candidates. However, we have requested permission to develop a new subaward to Dr. Christian Kastrup at the University of British Columbia (in Vancouver, Canada), and we are now awaiting permission to enact this subaward. When he was previously working with Dr. Ismagilov's lab, Dr. Kastrup developed the microfluidics-based approach that defined the spatial threshold nature of activators of blood clotting and he is particularly well qualified to carry out the analyses of our TSPs. (Importantly, Dr. Kastrup currently has these techniques already up and running in his laboratory, so there should be minimal further delays in carrying out these needed tests of TSPs.) We are hopeful that the subaward will be approved soon. In the meantime, the Kastrup and Ismagilov labs are continuing their previously ongoing collaborations (which are not yet funded by a

subaward to Dr. Kastrup), some of which are summarized below wherever the topic of that collaboration is germane to the present project. When the subaward to the University of British Columbia is approved, then Dr. Kastrup will be able to begin actual funded studies under this project.

***Human Anatomical Substances use approval (Milestone #2)*** — Some of the studies to be conducted in Dr. Ismagilov's lab employ blood samples from human volunteer blood donors, which requires regulatory approval. Dr. Ismagilov obtained IRB approval from Caltech for these studies (RI-334, approved on December 5, 2011) and this was communicated on Thursday, December 8, 2011 to Ms. Brigit Ciccarello (Regulatory Compliance Specialist, Telemedicine & Advanced Technology Research Center, U.S. Army Medical Research and Materiel Command, Fort Detrick, Maryland), who submitted the necessary documents to obtain approval from the Office of Research Protections. Dr. Ismagilov was notified on March 20, 2012 that the protocol has been approved by the Office of Research Protections. IRB protocol 12502A at the University of Chicago, which conferred approval on the Ismagilov lab's work on the project prior to their move to Caltech, was closed on March 2, 2012. Thus, the subaward agreement has been implemented at Caltech and the necessary human subjects regulatory approvals have been obtained at Caltech.

## **Scientific Progress**

### **BACKGROUND**

Inorganic polyphosphate (polyP) is a linear, unbranched polymer composed of orthophosphate monomers. Extremely conserved and ubiquitous across a diverse range of organisms, its physiological function in humans and other complex eukaryotes has only recently been broadly elucidated [1]. PolyP is secreted from the dense granules of activated platelets and acts at various stages of the coagulation cascade depending on its polymer length [2].

Long-chain polyP (generally greater than 500 phosphate monomers long) serve as potent contact surfaces for initiation of the intrinsic pathway, while shorter polyP polymers of 60-100 phosphate units catalyze the conversion of the zymogen Factor V to its active form and slow the breakdown of fibrin clots [2, 3]. With its role now clearly established as a critical hemostatic agent within the body, polyP could potentially serve as a useful and safe procoagulant compound to address multiple bleeding disorders including internal hemorrhage.

When intravenously administered, nanoparticle therapies have been devised to target activated platelets with some success, but the goal of functionally delivering a procoagulant therapy to treat internal hemorrhage in practice has yet to be fully realized [4]. We are developing novel approaches for the targeted delivery of nanoparticles functionalized with controlled amounts of polyP. These tunable particles will then be able to selectively target sites of injury in response to appropriate stimuli such as a drop in temperature without the induction of clotting anywhere else in the body, a property that aqueous polyP unfortunately does not possess. Therefore, the goal of this study is to understand the process of particle-induced blood clotting, which could eventually lead to optimally engineered particles for coagulation.

### **A. Studies in the Morrissey lab (toward Task 3, Milestone 4)**

The Morrissey lab has successfully developed highly scalable methods for reproducibly size-fractionating polyP in gram quantities, which has facilitated efforts in the Stucky and Liu labs to formulate various polyP-bearing nanoparticles.

We previously published that the zero-length crosslinking agent, N-(3-Dimethylaminopropyl)-N'-ethylcarbodiimide hydrochloride (EDAC), can promote the formation of covalent phosphoramidate linkages between the terminal phosphates of polyP and a variety of primary amine-containing organic compounds [5]. This covalent linking chemistry has served as the basis for the production of many of the nanoparticles being used at all four sites in this project, so we wanted to understand the stability of phosphoramidate linkages to the terminal phosphates of polyP, and in particular we were concerned that the linkages might prove to be acid-labile. Accordingly, we investigated the long-term stability of

polyP containing phosphoramidate linkages and confirmed the acid-lability of such linkages (Figure1). These results indicate that the best storage condition for phosphoramidate labeled polyP is pH 8.

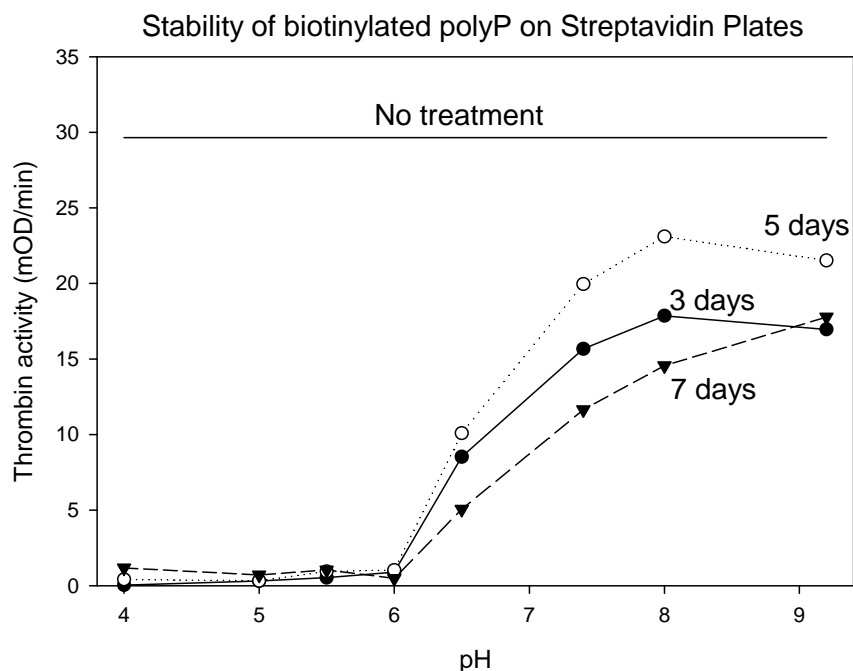


**Figure 1.** Effect of storage pH on the stability of phosphoramidate linkages between polyP and an amine-derivative of biotin. PolyP containing terminal biotin moieties attached via phosphoramidate linkages were captured on immobilized streptavidin and then stored for 3 to 7 days at the indicated pH values. The wells were washed and then the ability of thrombin to bind to the immobilized polyP was used to detect the amount of polyP remaining attached to the wells. The results show that the phosphoramidate linkage is acid-labile, and that the linkage has greatest stability when stored in solution at pH 8.

Although coupling of polyP to primary amines is highly reproducible in our hands, we wished to expand the coupling chemistries available to create stable, covalent linkages to the terminal phosphates of polyP. We have now identified coupling conditions using EDAC that allow the efficient coupling of a variety of alcohols to the terminal phosphates of polyP via ester linkages.

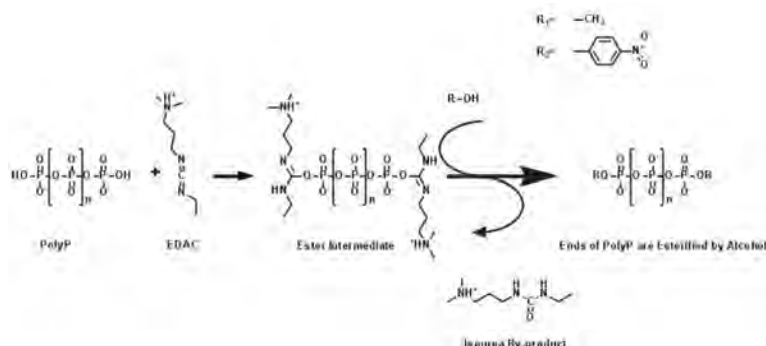


**Figure 2.** Coupling chemistry to prepare ester linkages to the terminal phosphates of polyP.

To date we have successfully coupled methanol and ethanol to the terminal phosphates of polyP, and in the case of couple of methanol, we have confirmed the quantitative derivatization of the terminal phosphates of polyP with methyl groups using NMR. We have also identified conditions that allow us to couple the yellow dye, *p*-nitrophenol, to the terminal phosphates of polyP via ester

linkages, in an EDAC-mediated reaction. As expected, the light absorption of the *p*-nitrophenol is shifted to the UV spectrum when coupled to polyP, and when an exopolyphosphatase such as alkaline phosphatase completely degrades polyP, it releases the *p*-nitrophenol as free dye, which returns to its intense yellow color. This has therefore allowed us to prepare chromogenic substrates for exopolyphosphatases and endopolyphosphatases that are present in a variety of biological samples.

Due to the presence of endo- and exopolyphosphatases, polyP has a half-life of approximately 90 min in blood or plasma [1, 6]. In order to make maximal use of nanoparticles containing polyP as their procoagulant payload, it is highly desirable to identify the enzyme(s) responsible for degrading polyP in vivo and to possibly determine strategies to protect circulating polyP on such nanoparticles. Using our novel, high-throughput assays for detecting and quantify endo- and exopolyphosphatases, we are working to identify the polyP-degrading enzymes in plasma and determine the best ways to protect polyP from degradation by such enzymes.

In more recent work, we have obtained evidence that it is possible to create mixed anhydrides between the terminal phosphates of polyP and organic acids (i.e., carboxylate groups). We are currently optimizing the conditions for creating these mixed anhydrides and will shortly be evaluating their stabilities relative to phosphoramidate- and ester-linked adducts attached to the terminal phosphates of polyP. And finally, we are actively investigating the possibility of covalently coupling thiols to the terminal phosphates of polyP.

## **B. Studies in the Ismagilov lab**

**Task 1: Conduct spatially-defined numerical simulations to identify threshold conditions. The simulations will utilize Comsol Multiphysics modeling software to screen concentrations of activators and particles, reaction rates, temporal dynamics, shear and external fields.**

**Year 2, subtask 1.a (Simulate mechanism 1: particles that alter local activity of blood):**

The Ismagilov lab's progress towards Milestone 1 is summarized in the preceding quarterly and annual reports. Postdoctoral scholar Stephanie McCalla and graduate student Travis Schlappi of the Ismagilov lab have joined the project, and they are working with Dr. Kastrup to identify simulation conditions and carry out the studies under this task.

Shear rate may be a threshold condition by which particles can aggregate and trigger blood clotting. To test this hypothesis, Dr. Kastrup's and Dr. Ismagilov's labs have designed several microfluidic devices with varying channel widths to test the effects that different shear rates have on clotting. To aid in experimental design and interpretation of results, the Ismagilov laboratory simulated the shear rate of fluid flow inside a microfluidic channel with a 500  $\mu\text{m}$  width 100  $\mu\text{m}$  height using COMSOL Multiphysics modeling software. As Figure 3 shows, as expected, the shear rate in the entrance region of the channel is different from that of the midplane (particularly in the corners). Thus, simulations will be used to design experiments and to interpret experimental findings of how shear affects coagulation.

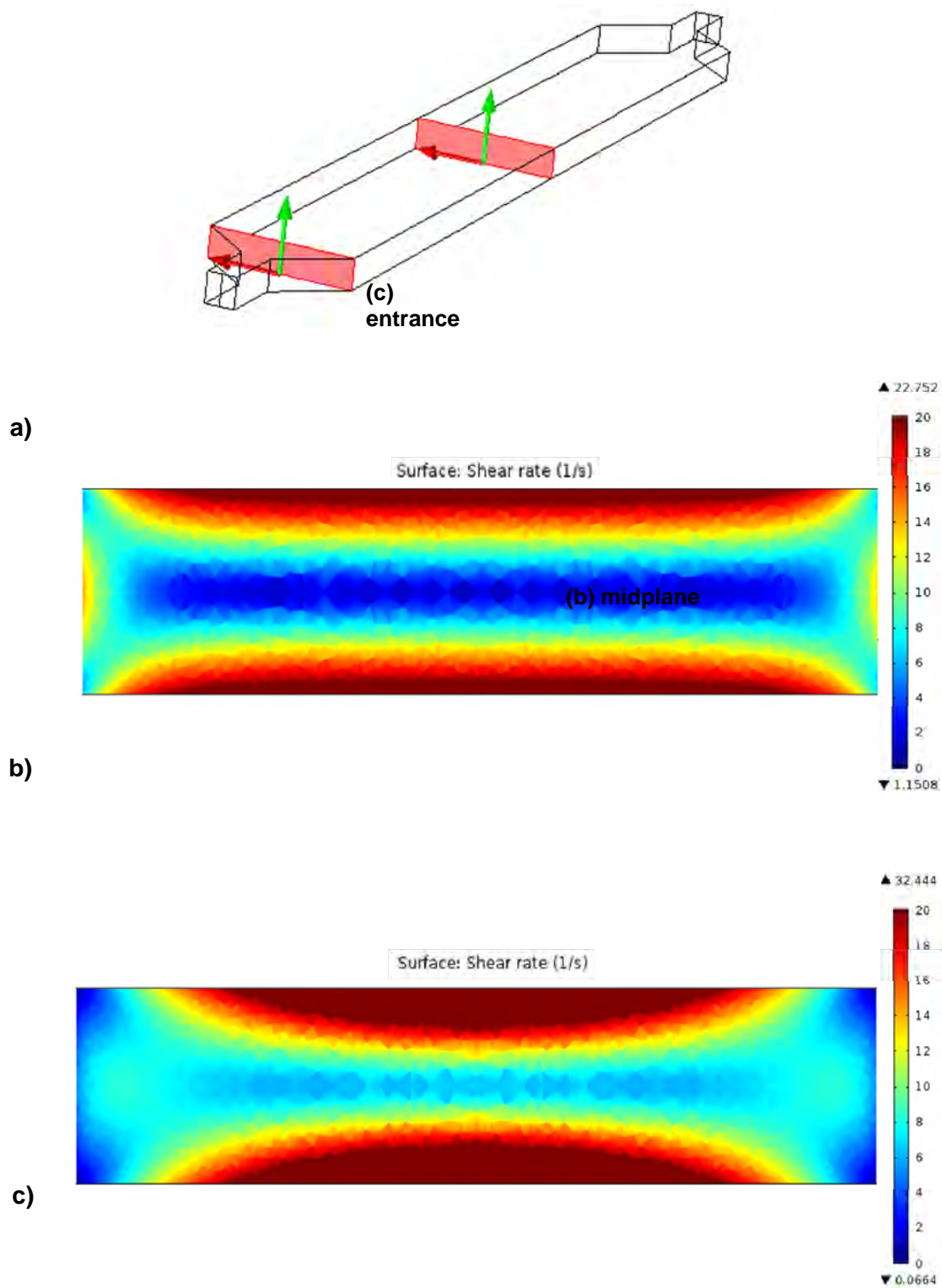


**Figure 3.** (A) Schematic of the microfluidic channel. (B) Shear rate simulation for the midplane of the channel, where different colors represent different shear rates. (C) Shear rate simulation for the entrance of the channel, where different colors represent different shear rates.



### **Year 2, subtask 1.b (Simulate mechanism 2: particles that generate large patches of activity):**

The Ismagilov lab's progress towards Milestone 1 is summarized in the preceding quarterly and annual reports. Postdoctoral scholar Stephanie McCalla and graduate student Travis Schlappi of the Ismagilov lab have joined the project, and it is anticipated that they will work together with Dr. Kastrup to identify simulation conditions and carry out the studies under this task in the near future.

### **Year 2, subtask 1.c (Simulate mechanism 3: particles that promote accumulation of activators):**

The Ismagilov lab's progress towards Milestone 1 is summarized in the preceding quarterly and annual reports. Postdoctoral scholar Stephanie McCalla and graduate student Travis Schlappi of the Ismagilov lab have joined the project, and it is anticipated that they will work together with Dr. Kastrup to identify simulation conditions and carry out the studies under this task in the near future.

### **Task 2: Conduct *in vitro* experiments to test recommended threshold conditions with human plasma and whole blood.**

#### **Year 2, subtask 2.a (Pattern patches of activator-generating precursors, activators, or sticky meshes on surfaces inside microfluidic devices):**

The Ismagilov and Kastrup labs developed a method for conducting *in vitro* experiments to test recommended threshold conditions of TSPs in a microfluidic chamber (Figure 4). The assay can determine the rate of clotting in response to local and total concentration changes of activators present in the device.

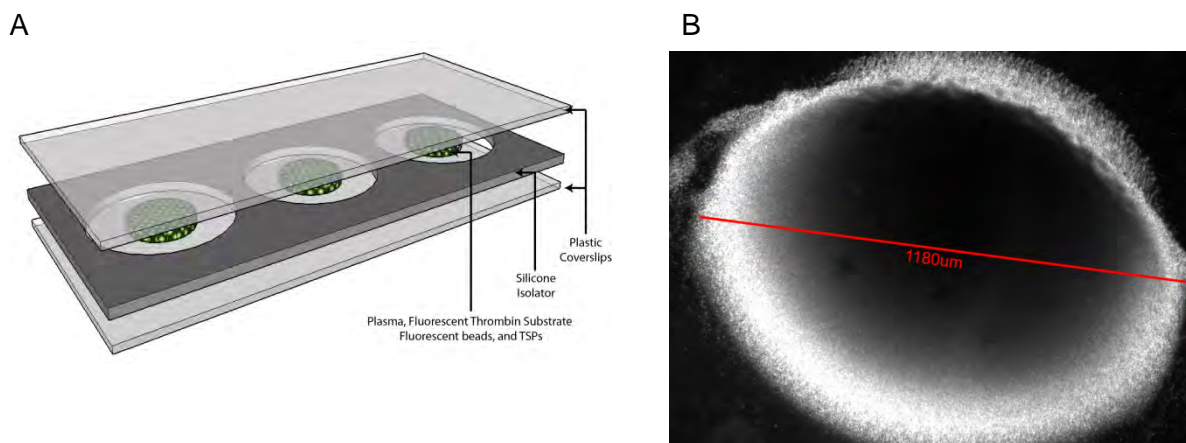


**Figure 4.** Microfluidic chamber assay for determining clotting in response to local activator concentration. (A) The formation of fibrin in  $< 5 \mu\text{l}$  of plasma is monitored by the movement fluorescent beads. (B) Silica nanoparticles (functionalized or unfunctionalized) can be clustered into small patches inside the chambers using a magnet, which allows comparison between clustered and non-clustered particles.

#### **Year 2, subtask 2.b (Test rate of blood clotting in response to these patches under varying fluid flow conditions):**

The Ismagilov and Kastrup labs tested if clustering of synthetic particles could switch plasma to a more procoagulant state. They found that when magnetic silica particles were clustered, the plasma rapidly clotted (Figure 5). But when the particles were evenly dispersed, the clot times were similar to

control samples without particles. This experiment confirms that synthetic nanoparticles can exhibit threshold-switchable behavior, which can be controlled by local concentration and clustering particles into patches. This effect is robust and also occurs in plasma that is depleted of a coagulation factor. Clotting of plasma deficient in coagulation factor XI, which mimics plasma from patients with hemophilia C or other bleeding disorders, is sensitive to the clustering of nanoparticles, and clots more rapidly when particles are clustered in a patch (Figure 3B).

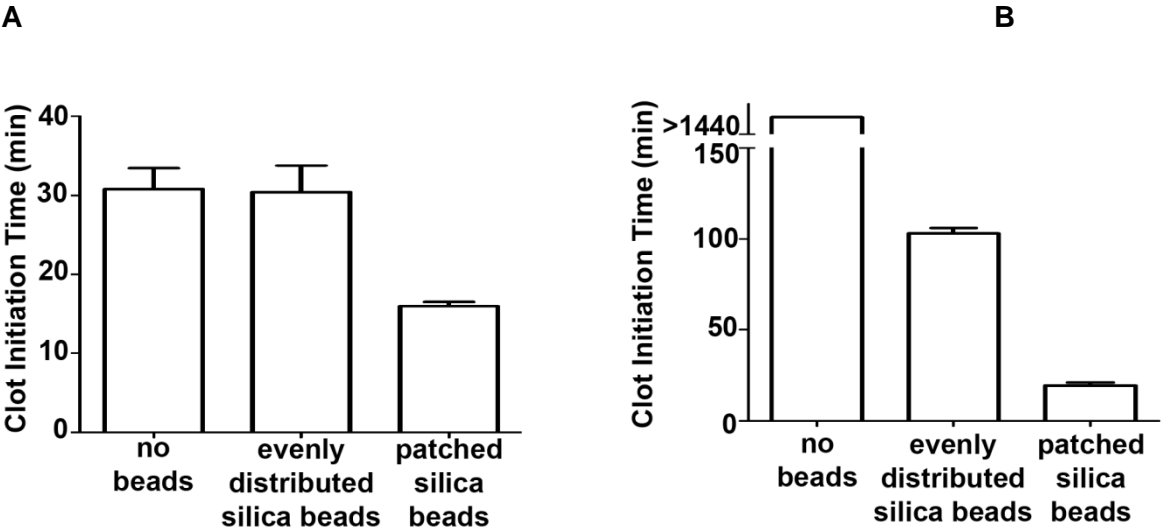


**Figure 5.** Initiation of clotting by nanoparticles is sensitive to clustering and local concentration of the particles. (A) Clot initiation time of normal human plasma (Panel A) and FXI-deficient human plasma (Panel B) in response to local concentration changes in silica as an activator.

In addition to silica particles, the Kastrup Lab had also conducted microfluidic chamber experiments using SNP-P70 particles synthesized by the Stucky group from 70 monomer polyP provided by the Morrissey group (Figure 6). The results confirmed findings from the Stucky Lab that the clotting rate is dependent on SNP-P70 concentration. This result, along with the results from Figure 2 above, suggests that SNP-P70 will demonstrate threshold-switchable behavior. This result also identified the appropriate concentrations of SNP-P70 to test in microfluidic devices mimicking hemorrhage, discussed further in Task 4.

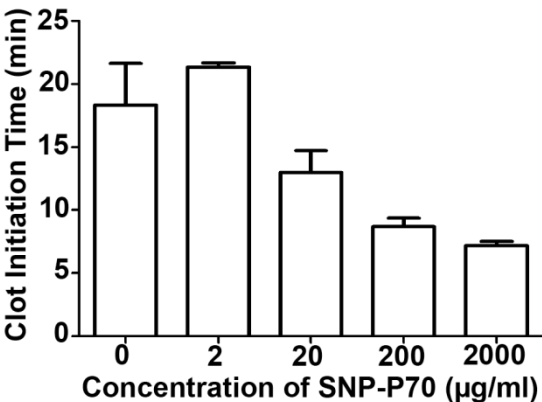


**Figure 6.** Clot initiation time of normal recalcified human plasma in response to total concentration changes in SNP-P70.

#### Task 4: Design and utilize microfluidic devices that reproduce shear flow and surface chemistries relevant to internal hemorrhage.

**Year 2, subtask 4.a (Design and test microfluidic devices that reproduce shear flow rates in arteries/veins; validate with existing knowledge of threshold effects on blood clotting; refine devices as needed):**

The Ismagilov lab and Kastrup lab have worked together to design microfluidic clot initiation experiments which would simulate the low shear conditions found in internal hemorrhage. Low shear is characteristic of internal hemorrhage where blood is either pooling or flowing into a space with large dimensions. In order to simulate these conditions, the microfluidic device depicted in Figure 5 was used. On the device are two inlet channels for citrated human plasma and calcium solution, which are mixed on chip in the “mixing region.” The device features two outlets – one narrow without deformations representing high shear and a second with small wells which serve as the region of lowest shear due to their enlarged size.

Using this device, Ismagilov lab and Kastrup lab have successfully demonstrated that clotting initiates at the regions of lowest shear in the microfluidic device. The first experiment sought to demonstrate that silica nanoparticles would initiate clotting faster than non-particulate controls and that the initiation would selectively occur at the regions of lowest shear. Magnetic silica particles were suspended in the calcium solution, which was mixed on-chip with citrated plasma achieving a final concentration of 200  $\mu\text{g/ml}$ . Lowest shear regions were imaged continuously by fluorescence microscopy over two hours. Clotting initiated exclusively in lowest shear regions at approximately 25 minutes. As a control, recalcified plasma containing no magnetic silica particles also initiated clotting in the regions of lowest shear but at 90 minutes. Here we have shown clotting selectively initiates at regions of low-shear using magnetic silica particles – which are known activators of clotting – which is validated by existing knowledge of threshold effects on clotting.

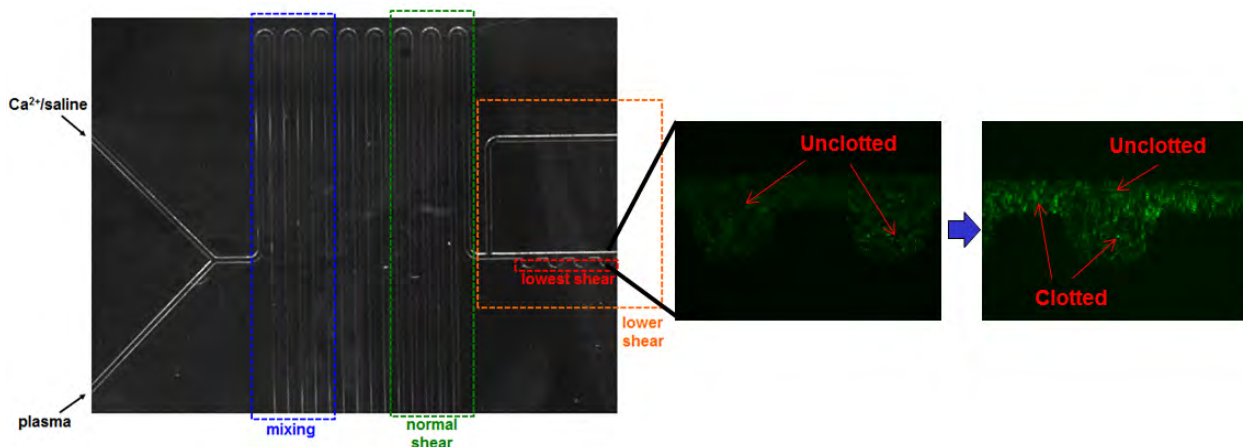


**Figure 7** Microscopy images of the first microfluidic device used for testing of low-shear clot initiation using magnetic silica particles. (left to right) (1) The microfluidic device including calcium-saline and plasma inlets, mixing regions, and regions of varying shear. (2) Fluorescence microscopy of unclogged plasma with green-fluorescent tracer beads in low shear region. (3) Fluorescence microscopy of low shear region showing clotted plasma.

The Ismagilov lab and Kastrup lab have designed new microfluidic devices that will enable the testing of a greater number and range of shear rates. The new designs also normalize the distance traveled by plasma to regions of varied shear as well as pressure drops across these regions. Using three new designs, known shear rates of 0.1 to 1200  $\text{s}^{-1}$  can be reliably achieved. Each device is able to test six different shear rates at once. Devices will also feature the same on-chip mixing of citrated

plasma and calcium solution as in the previous design. Photolithographic masks have been produced and PDMS molds are currently being fabricated for these device designs.

**Year 2, subtask 4.b (Use these devices to test whether TSPs initiate coagulation specifically at the site of “bleeding” and not elsewhere):**

The Ismagilov lab and Kastrup lab have worked together to design microfluidic clot initiation experiments which would simulate the low shear conditions found in internal hemorrhage and test the clotting activity of SNP-P70 TSPs under these conditions. If SNP-P70 TSPs can be shown to initiate clotting selectively at regions of low shear, this would suggest that they would also selectively initiate clotting at sites of internal hemorrhage where shear is also low. SNP-P70 TSPs have been successfully shown to selectively initiate clotting at sites of low shear. The experiment used to demonstrate this is the same as that which is outlined for subtask 4.a but with SNP-P70 particles in place of magnetic silica particles. Concentration of particles, flow rates and imaging times were the same as in subtask 4.a. Clotting initiated in regions of lowest shear at approximately 22 minutes. Clot initiation times for magnetic silica particles, SNP-P70 and no-particle control are shown in Figure 6. These results were consistent with findings of the microfluidic magnetic silica experiments of subtask 4.a and demonstrate the selective clotting of plasma by SNP-P70s at low shear.

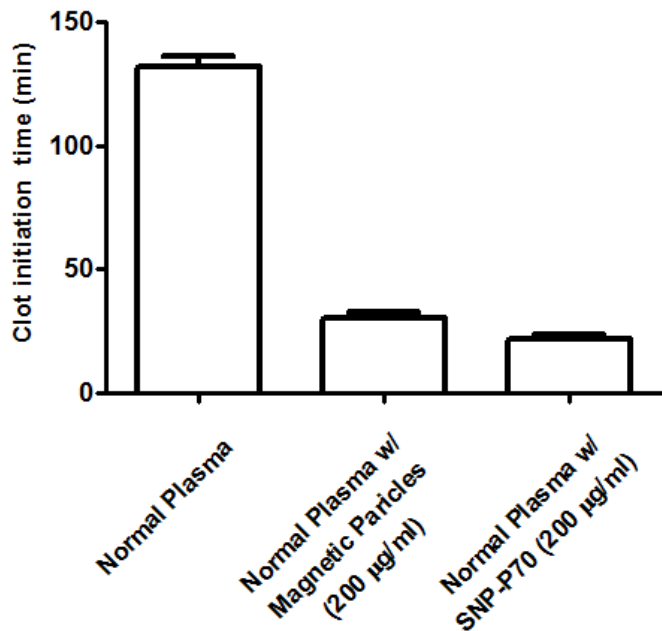


**Figure 8.** Clot initiation times for microfluidic testing of shear-responsive TSPs. n=3

SNP-P70 shear-responsiveness experiments will also be repeated in the new microfluidic devices described under subtask 4.a.

**Year 2, subtask 4.c (Use these results to inform refinement of models in Aim 1 and of particles in Aim 2, before particles are ready to be used in animal models):**

The Ismagilov lab and Kastrup lab together have achieved preliminary results regarding clot initiation under low shear flow, mimicking shear conditions similar to those found in internal hemorrhage. Currently, it has been seen that magnetic silica particles and SNP-P70 are capable of selectively initiating clotting at regions of lowest shear in the microfluidic model, as shown in the two preceding figures. This initiation was achieved at particle concentrations of 200 µg/ml. The clot initiation by TSPs was seen at approximately 25 min as opposed to 90 min in controls. This data on particle

concentrations and clot initiation times will be used in the refinement and verification of models in Aim 1 and of particles in Aim 2 during the next quarter.

### C. Studies from the Liu lab

#### Nanoparticle Synthesis at Physiological Salt Concentrations (Toward Task 3, Subtask c)

Throughout the past year the Liu Group has primarily focused on developing polyphosphate nanoparticles through nanoprecipitation.

Initially, intermediate chain length polyphosphate (polyP250) and the biocompatible copolymer *poly(lactic-co-glycolic) acid* (PLGA) were coprecipitated using traditional and flash nanoprecipitation. The scheme for traditional precipitation was as follows: PLGA in THF was added directly to a mixture of polyphosphate in 100 mM NaCl, resulting in PolyP-PLGA nanoparticles after the addition of more water. The flash nanoprecipitation technique using a multi-inlet vortex mixer is outlined in **Fig. 9**. Both techniques resulted in relatively low nanoparticle formation efficiencies (~30%) and high polydispersity (**Fig. 10**). Moreover, polyphosphate still nanoprecipitated without the presence of PLGA.

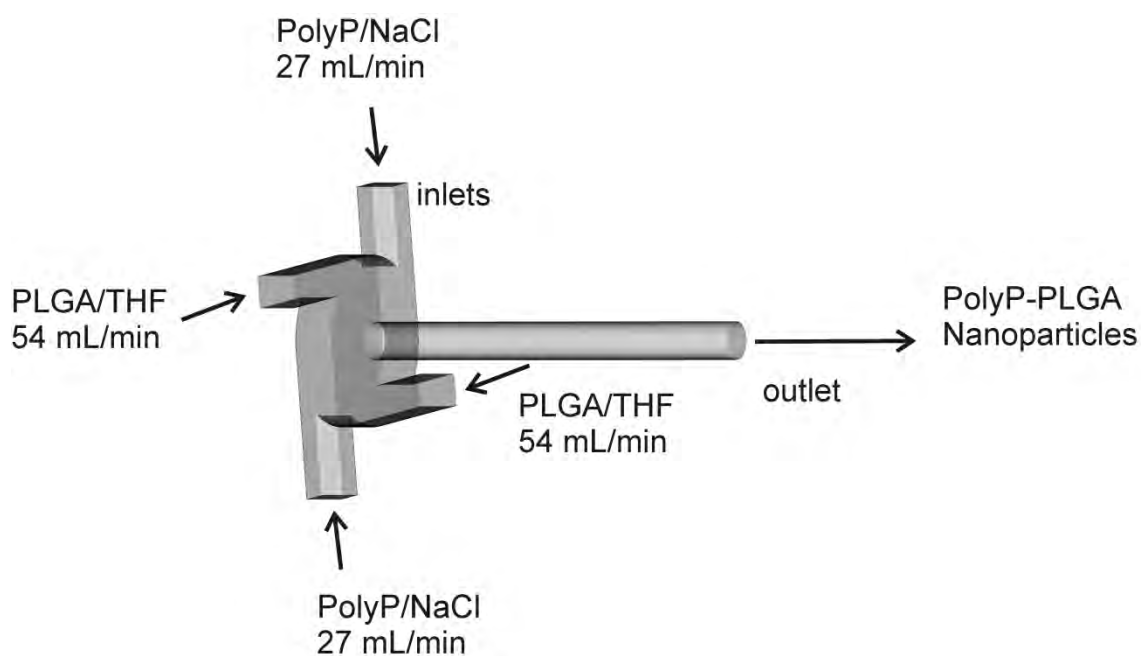


**Fig. 9.** Flash nanoprecipitation of polyphosphate with MIVM. PolyP and PLGA were coprecipitated in a multi-inlet vortex mixer (MIVM), which mixes the inlet streams at high Reynolds number, ensuring thorough mixing of the reactants.

Sample	PolyP Encapsulation (%)	Size (nm) by Volume	Polydispersity
PolyP Particle Hand Mixing	32.3	383.9	0.367
PolyP-PLGA 2:1 Hand Mixing	33.1	528.4	0.381
PolyP-PLGA 1:1 Hand Mixing	21.4	253.8	0.285
PolyP Particle Flash Precipitation	23.9	154.0	0.312
PolyP-PLGA 1:1 Flash Precipitation	29.6	218.0	0.304

**Fig. 10.** PolyP Particle Characteristics. PolyP250 encapsulation efficiency and PolyP-PLGA particles average size, and polydispersity. Mixing kinetics (hand mixing vs. flash nanoprecipitation) has limited effect on the resulted particles. The PolyP encapsulation efficiency is close to 30% for all particles.

Once the candidate nanoparticles were synthesized using traditional and flash nanoprecipitation methods as outlined above, their procoagulant ability was determined by a microplate-based absorbance assay, which measures the turbidity of the clotting samples at 405 nm over time. The absorbance traces were fitted to a generalized Boltzmann logistic function, and the clotting time was arbitrarily defined as the time of inflection of the fitted curve. In **Fig. 11** below, the nanoparticles were tested at two different monophosphate concentrations at room temperature without preincubation with polyphosphate before recalcification. It is important to note that the Morrissey Group generally pre-incubates citrated plasma with polyphosphate before recalcifying because it was found to decrease clotting times. At 25  $\mu$ M, there is no statistically significant difference between the nanoparticles, polyphosphate, and positive control. At 2.5 mM monophosphate, two orders of magnitude higher, there is a statistically significant decrease in the coagulation time between PolyP particles, PolyP-PLGA particles and free PolyP from the positive control. Interestingly, PolyP particles had statistically identical clotting times to free PolyP, suggesting to the Liu Group that PolyP may be precipitating into nanoparticles upon recalcification. The average maximum turbidity was also determined for the clotting test at 2.5 mM MonoP. Smith *et al.* has shown that intermediate chain length polyphosphate (used here to make the nanoparticles) strengthens fibrin clot architecture, although the mechanism by which this enhancement occurs remains to be thoroughly elucidated.<sup>1</sup>

<sup>1</sup> Smith *et al.* "Polyphosphate enhances fibrin clot structure." *Blood*, **112**(7): 2810-2816

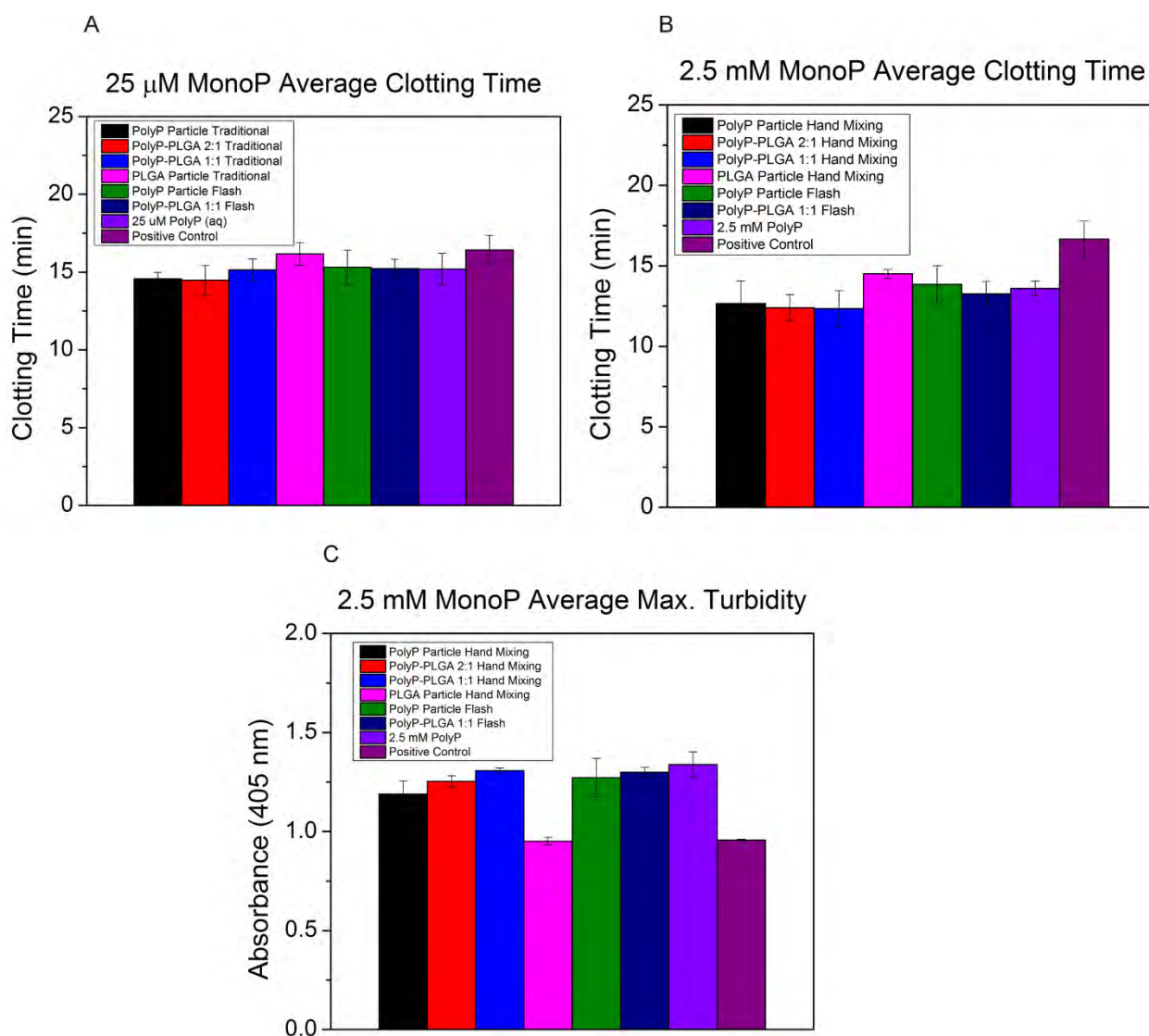


**Fig. 11.** (A) Average clotting times of the PolyP-PLGA nanoparticles at 25  $\mu$ M MonoP. There is no statistically significant difference between the nanoparticle samples and the positive control. (B) Average clotting times of the PolyP-PLGA nanoparticles at 2.5 mM MonoP. The free PolyP and the PolyP and PolyP-PLGA nanoparticles clot significantly faster than the positive control. (C) Average maximum turbidity at 2.5 mM MonoP. Plot showing the average maximum turbidity of the samples, representing the density and crosslinking of the polymerized fibrin clot. Polyphosphate is known to drastically enhance fibrin clot architecture, although its mechanism is not yet understood.

The ability of polyphosphate to spontaneously nanoprecipitate in the presence of ionized sodium served as an impetus for the Liu Group to identify other suitable cations which could precipitate polyphosphate with higher nanoparticle formation efficiency and lower polydispersity. It has been known for decades that polyphosphate reversibly binds calcium, magnesium, manganese, and other metal ions<sup>2</sup>. The dissociation constants for calcium and magnesium have even been quantified in the literature<sup>3</sup>. Calcium is a natural choice since the dissociation constant is relatively low. Moreover,

<sup>2</sup> Kornberg, A. "Inorganic Polyphosphate: Toward Making a Forgotten Polymer Unforgettable." *Journal of Bacteriology*, **177**(3), 1995: 491-496

<sup>3</sup> Bonting, CFC *et al.* "The elemental composition dynamics of large polyphosphate granules in *Acinetobacter* strain 210A." *Archives of Microbiology*, (1993), **159**: 428-434.



calcium plays a central role in the intrinsic pathway of coagulation. In addition to serving as an essential cofactor for tenase and prothombinase complex formation, calcium could potentially precipitate polyphosphate, forming nanoparticles that could serve as negatively charged surfaces for FXII activation.

Supporting this hypothesis, it was discovered that polyphosphate spontaneously nanoprecipitates in aqueous solutions containing concentrations of ionized calcium and magnesium cations naturally found in human circulation. Dynamic light scattering (DLS) was employed to determine the solubility of polyphosphate chains of various polymer lengths. Analogous to determining the critical micelle concentration of surfactants in suspension, the scattering intensity should markedly increase once the polymer coalesces into nanoparticles. Nanoparticle formation efficiency of very long chain polymers (e.g. PolyP>1000) is much higher and very robust compared to platelet polyP (polyP70). The addition of monovalent cations such as Na<sup>+</sup> and K<sup>+</sup> at physiologic concentrations had little effect on polyphosphate solubility (**Fig. 12**).



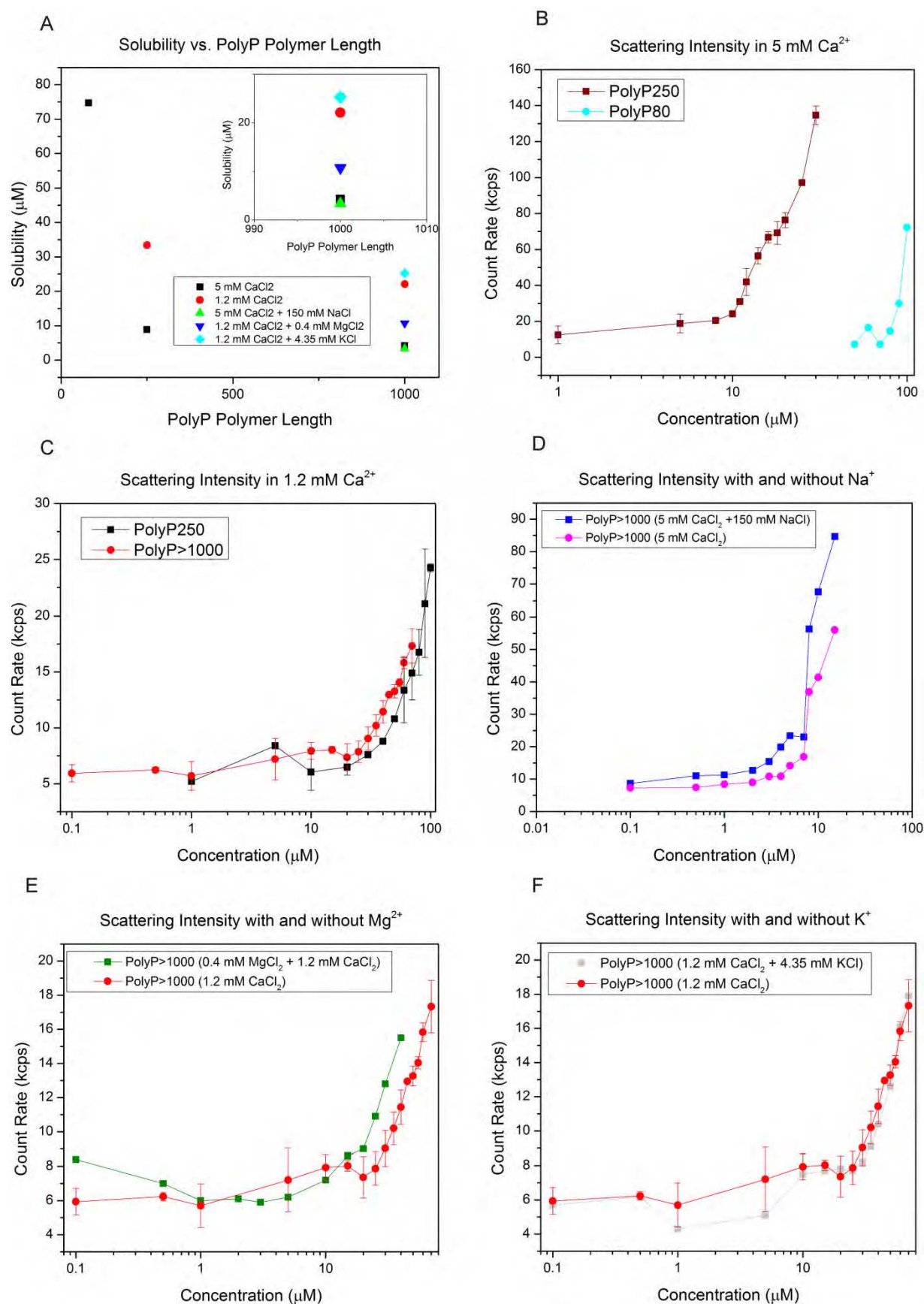


**Fig. 12.** (A) Solubility of polyphosphate vs. polymer length. solubility of polyphosphate of different polymer lengths in the presence of divalent metal cations (e.g.  $\text{Mg}^{2+}$  and  $\text{Ca}^{2+}$ ) at biologically relevant

concentrations. The presence of monovalent ions (e.g.  $K^+$  and  $Na^+$ ) at physiological concentrations exerted little precipitatory effects. (B) Longer polymer chains are less soluble in 5 mM  $Ca^{2+}$ . DLS measurements for polyP250 and polyP80 in the presence of 5mM  $CaCl_2$ . The transition points are decided to be the solubility of the polyP. (C) Bacterial PolyP has high nanoparticle formation efficiency compared to shorter chain lengths. DLS intensity of polyP250 and polyP1000 in the presence of 1.2 mM  $CaCl_2$ . (D) Addition of 150 mM  $Na^+$  exerts little precipitatory effects in the presence of 5 mM  $Ca^{2+}$ . The solubility of polyphosphate does not change appreciably at plasma's ionic strength of 150 mM in the presence of 5 mM  $Ca^{2+}$ . (E) Magnesium works synergistically with calcium to precipitate polyphosphate. Addition of physiological amounts of ionized magnesium decreases the solubility of polyP1000 approximately two fold. (F) Addition of potassium does not change polyphosphate's nanoparticle formation efficiency. Physiological amounts of  $K^+$  have no effect on the solubility of polyP1000.

### Polyphosphate Particle Growth Kinetics

The polyphosphate nanoparticles were further characterized by determining their initial mean hydrodynamic diameter and their growth kinetics over a time scale relevant for hemostatic and hemorrhagic events. *A priori* one would expect polymer chain length to dictate nanoparticle size; however, this does not seem to be the case. As shown in in **Fig. 13A**, the major factor driving nanoparticle diameter is the calcium:polyphosphate stoichiometry. At excess levels of  $Ca^{2+}$  routinely used in clotting assays (5 mM), the average effective diameter for all three polyP (polyP45, polyP70, and polyP250) is approximately 150-200 nm. At physiological levels of ionic calcium (1.2 mM), the mean effective diameter polyP250 is approximately 50 nm. **Fig. 13B** shows the particle growth kinetics for four paradigmatic polymers (45-, 70-, 250-, and >600-mer) at 5 mM  $Ca^{2+}$ . The particles are metastable for tens of minutes and then explosively agglomerate to micron-sized particles without any known induction. This explosive growth occurs on a time scale that is roughly equivalent with the time it takes for the induction of clotting factors during a bleeding event. This behavior requires further investigation as metastable nanoparticles normally manifest gradual aggregation behavior over time unless there are changes in pH, temperature, or ionic strength etc., depending upon the chemistry of the colloidal dispersion.

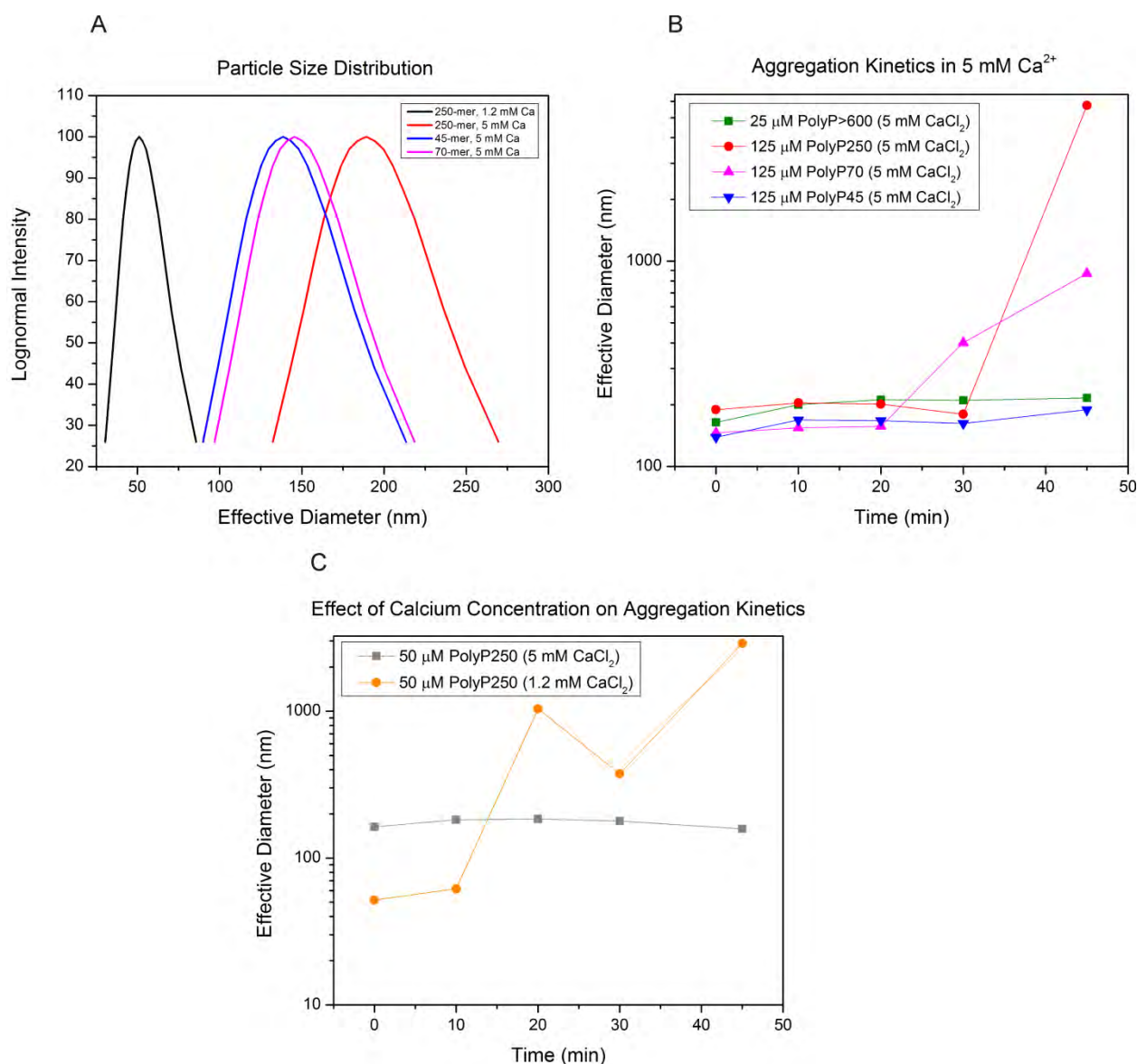


**Fig. 13.** (A) Particle size distribution of polyphosphate of various chain lengths at low and high calcium concentration. Mean initial hydrodynamic diameter of the nanoparticles of polyP45, polyP70, and polyP250 at two different calcium concentrations. The monoP concentration is kept constant at 125 μM. The calcium:polyphosphate ratio has bigger effect on nanoparticle size, rather than the polymer length. (B) Particle Growth for PolyP NPs at 5 mM Ca<sup>2+</sup>. Growth kinetics of the nanoparticles of polyP45, polyP70, polyP250, and polyP600) at 5 mM Ca<sup>2+</sup>, the concentration normally encountered in standard clotting assays. The particles remain the same size for approximately 20 to 30 minutes, then explosively agglomerate to micron-sized particles. (C) Effect of calcium concentration on particle growth kinetics. Maintaining the same monophosphate concentration and decreasing the ionized calcium concentration to match the levels found in human plasma (1.2 mM), the polyphosphate particles aggregate within 10 to 20 minutes.

In addition to studying polyphosphate's solubility and characterizing its aggregation kinetics, DLS was also used to ascertain if there was any hysteresis in polyphosphate nanoparticle formation. As done previously the solubility was determined for polyP250, in 5 mM Ca<sup>2+</sup>. Once it was established that the solubility of this polymer was 8.84 μM at this salt concentration, a sample well above the

solubility concentration (in this case 30  $\mu\text{M}$ ) was diluted progressively with more buffer (5 mM  $\text{CaCl}_2$ ) to decrease the polyphosphate concentration and keep the calcium concentration constant, and then the scattering intensity was measured after each dilution. As can be seen in **Fig. 14**, the system exhibits hysteresis: the count rate remains much higher even below the solubility concentration despite a thermodynamic driving force for some of the particles to re-dissolve. Evidence that polyphosphate nanoparticle formation manifests hysteresis has potentially profound ramifications: for example, a fatal scenario could be envisioned in which a pathogenic bacterium could locally secrete polyphosphate nanoparticles at high concentrations at the site of infection which would subsequently be distributed throughout the circulation via convection and diffusion, maintaining its nanoparticle format and associated biological functionality (e.g. as a proinflammatory and procoagulant agent) throughout the body due to hysteresis.

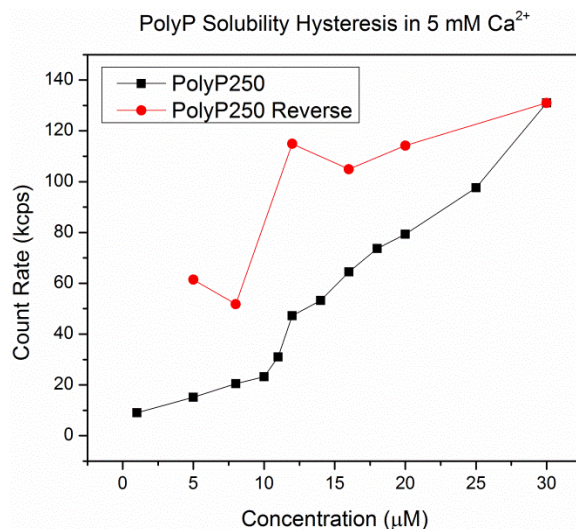


**Fig. 14.** DLS intensity of polyP250 at various concentration in the presence of 5mM  $\text{CaCl}_2$ . The black curve is for gradually increasing polyP concentration and the red one is for diluting polyP starting from 30 mm. . Solubility of polyP250 with 5mM  $\text{CaCl}_2$  is previously determined to be 8.84  $\mu\text{M}$ .

#### Characterization of Coagulation under Flow Conditions (Toward Task 4)

In addition to synthesizing candidate threshold-switchable polyphosphate nanoparticles, the Liu Group has devised a novel method to measure the coagulability of human plasma subject to shear flow via modification of a technique commonly used in the rheology community called capillary pinch-off. A device was fabricated to monitor the dripping of recalcified human plasma out of a micron-sized diameter capillary tube with the aid of high-speed imaging. Capillary, viscous, viscoelastic, and gravitational forces all contribute to pinch-off dynamics. With the addition of calcium and the induction of the contact pathway, plasma's rheological properties change significantly: initially, plasma is a Newtonian fluid with physical properties such as viscosity and surface tension close to that of water. However, after several minutes, fibrinogen is transformed into fibrin and begins to polymerize and cross-link and the fluid begins to gelate. Moreover, the viscosity increases by orders of magnitude. Capillary pinch-off allows the investigator to directly observe this gelation transition and calculate the clotting time by measuring the dimensionless length of the neck just prior to pinch-off. As the extensional viscosity increases, the neck gets longer and longer. **Fig. 15** shows a montage of a representative capillary pinch-off experiment with recalcified plasma and phospholipids. At approximately 30-35 minutes, the length of the neck increases significantly and the fluid transitions

into a gel-like state. This time roughly corresponds with the partial thromboplastin time (PTT), a common clinical diagnostic test used to measure activation of the contact pathway.

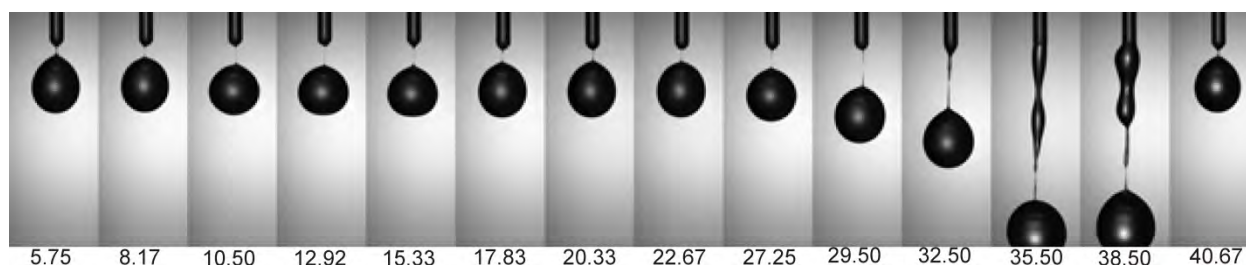


**Fig. 15.** Capillary Pinch-Off Montage. Representative experiment showing the change in the fluid characteristics of blood plasma as it coagulates. The neck at pinch-off gets progressively larger until the plasma resembles a thick gel. The time to gelation agrees with other established methods like PTT. (Time below montage in minutes.)

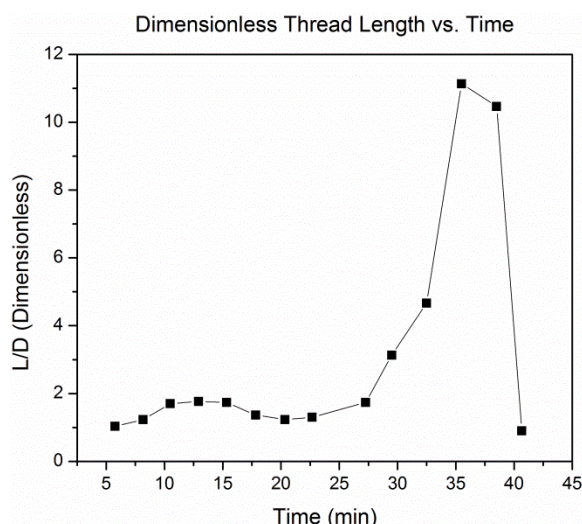


**Fig. 16.** Dimensionless neck length vs. time. Plot of the dimensionless length versus time for the same experiment as above in **Fig. 15**. The dimensionless length was defined arbitrarily to be the length of the neck in pixels divided by the diameter of the tubing in pixels, as calculated by ImageJ Software.

Since plasma is coagulating as it is dripping from the capillary, a careful analysis of the pinch-off dynamics must also consider the effects of the multiple enzymatic and polymerization reactions on the rheological/flow properties of the fluid. For instance, Teflon, a relatively inert fluorohydrocarbon, was chosen as the material for the capillary. It was noticed, however, that if the infusion rate (dripping flow rate) was too low, fibrin clots begin to deposit on the tube lumen, and a gel is not detected dripping from the capillary throughout the course of the experiment even though clotting has certainly occurred. To circumvent this problem, the plasma is continuously mixed while it is not dripping from the capillary at sufficient shear rates to minimize fibrin deposition. However, if the mixing flow rate is too high, the three-dimensional fibrin gel is sheared apart, completely changing its rheological properties. Colace and Diamond constructed a phase diagram relating fibrin clot architecture and morphology and divided into three regimes: a 3-D gel, 2-D mat, and a 1-D thin film. They determined that the critical parameters determining fibrin clot structure were the Péclet number, relating convective and diffusive transport, and the Damköhler number, relating the reaction rate (fibrin monomer to polymer) to diffusion. Increasing the mixing rate increases the Péclet number<sup>4</sup>. **Fig. 17**

<sup>4</sup> Colace et al. *Microfluidics and Coagulation Biology*. **Annu Rev Biomed Eng.** 2013(15): 283-303.



shows a phase diagram which the Liu Group constructed by numerous experimental trials at various infusion and mixing conditions. Only one pair of mixing and infusion rates so far has been determined to yield observation of gelation. In the future, the Liu Group will continue to elucidate plasma dripping and gelation through the identification of critical physical parameters/ dimensionless groups (through both simulation and experiment) such as pre-shear/mixing rate, the Weber and Ohnesorge numbers traditionally used in pinch-off analyses, and the Péclet and Damköhler numbers previously investigated by Colace and Diamond.

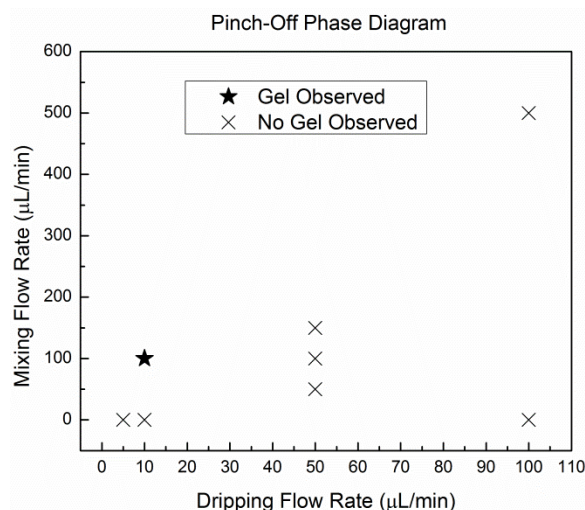


**Fig. 17.** Capillary Pinch-Off Phase Diagram. This plot was constructed to aid in the identification of important physical parameters in blood plasma pinch-off dynamics. In order for gelation to be observed, the infusion flow rate has to be low enough to be outside of a jetting regime, while the mixing rate has to be substantially high in order to minimize fibrin gel deposition on the tubing.

#### Future Work in the Liu Lab

- Measure growth kinetics of polyphosphate in BSA suspensions containing calcium to mimic human serum
- Encapsulate polyphosphate nanoparticles synthesized at high calcium concentration (5 mM  $\text{Ca}^{2+}$ ) into unilamellar lipid vesicles that are colloidally stable in normal physiological condition, but quickly release polyP at the bleeding sites.
- Synthesize phospholipid-polymer hybrid vesicles that have long half-life in circulation but are sensitive to inflammatory agents locally present at high amounts near trauma<sup>5</sup>.
- Work with Ismagilov, Kastrup and Morrissey labs to test the clotting activity of the particles in microfluidic devices.

<sup>5</sup> Andresen, Thomas L. "Advanced strategies in liposomal cancer therapy: Problems and prospects of active and tumor specific drug release." *Progress in Lipid Research*, **44** (2005): 68–97

## D. Studies from the Stucky lab

**Year 02, Task 3 — Design and test particles that will function as candidate TSPs. SUBTASK 3.a Develop candidate nanometer- and micron-scale particles for suitability for supporting TSPs; in particular, identify particles that do not trigger clotting when finely dispersed in plasma/blood. Months 4-6.**

Research in the Stucky group continues to focus on polyphosphate-functionalized silica (SNP-polyP) nanoparticles as the most promising TSP candidate for activating coagulation in internal injuries. As previously discovered, the ideal SNP-polyP candidate uses roughly 70 monomer polyP provided by the Morrissey group to synthesize SNP-P70. The ideal concentration for minimizing clot time is around 0.25 mg/ml, though the clot time remains under 2 min for concentrations as low as 0.05 mg/ml SNP-P70. Below 0.05 mg/ml, the concentration is too low to robustly activate coagulation. In addition to our research in Q1, the Stucky and Morrissey groups have filed a patent application for the SNP-P70 system.<sup>6</sup>

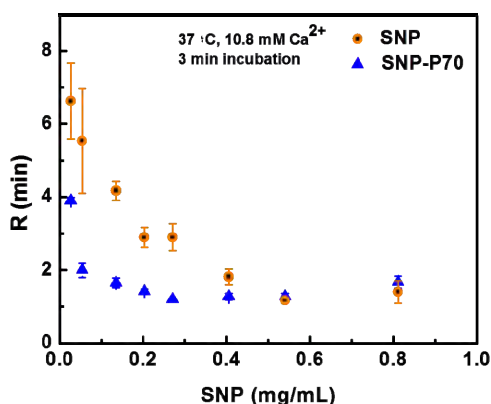


**Figure 18 - Clot time in plasma of SNP-P70 and bare SNP. Above 0.05 mg/ml, the SNP-P70 clot time is under 2 min.**

At the February project meeting at Caltech, the Ismagilov, Liu, Morrissey and Stucky groups met and discussed ideas to improve the deprotection and targeting of the SNP-P70 TSP. Protecting the particle enables it to be injected into the bloodstream without reaching the coagulation threshold in healthy vessels. In wounded vessels, the particle activates and accumulates in large enough concentrations to reach the threshold locally and induce coagulation at the wound site. Currently, our design uses an APTES bridge and a peptide sequence to link the nanoparticle to the protecting polyethylene glycol (PEG). The peptide contains an IEGR sequence that can be cleaved by FXa, a procoagulant factor with nanomolar concentrations at the wound site. In discussions with the Morrissey group, it was suggested that thrombin may be better suited for targeted cleavage as it is found in higher concentrations than FXa. We are looking to replicate the TSP system with a thrombin-cleavable peptide and to test the TSP's efficacy under static and flow conditions in the future.

**Year 02, Task 3 — Design and test particles that will function as candidate TSPs. SUBTASK 3.b Develop and refine procedures for chemically (covalently) attaching molecules that can trigger or enhance blood clotting (polyphosphate, tissue factor, etc.) to solid supports. Months 4-6.**

Previously, we have shown that bare silica nanoparticles can be functionalized with a targeting peptide and polyethylene glycol (PEG) to protect the molecule from clotting in healthy vessels (Figure 2). During Q2, we are testing the same strategy with the SNP-P70 system. The addition of P70 complicates functionalization. First, the amine terminal on APTES and the negative P70 chain can interact electrostatically to cause significant aggregation. Second, the APTES functionalization must

<sup>6</sup> UC Case 2013-559 titled "POLYPHOSPHATE-FUNCTIONALIZED INORGANIC NANOPARTICLES AS HEMOSTATIC COMPOSITIONS AND METHODS OF USE," submitted March 8, 2013.

be conducted using ethanol as a solvent; ethanol strips P70 off the SNP-P70 particles. Initial tests have shown that attaching P70 after functionalizing silica (SNP-APTES-P70) allows for successful functionalization with minimal aggregation. We aim to refine the SNP-APTES-P70 in the coming quarters to successfully protect and target the SNP-P70 system for internal use.

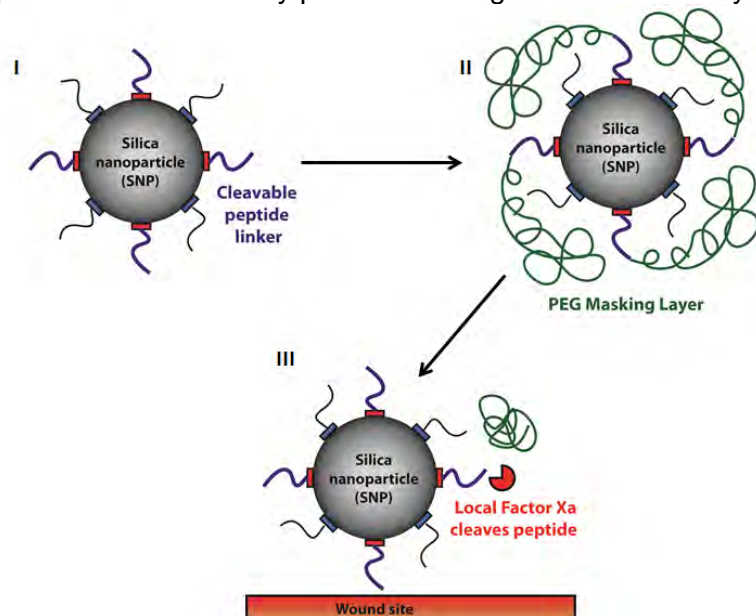


**Figure 19 - I) TSP with peptide linker that cleaves at wound site; II) PEG masking layer protects TSP from clotting in healthy vessels; III) At injury site, the peptide is cleaved, PEG layer released and the TSP activates to accelerate clotting.**

During Q2, we've tested the P70 functionalization on hydroxyapatite. While more complicated than silica, we were able to synthesize HA particles below 200 nm. The HA samples carried a slightly negative surface charge compared to silica, which prevents activation of the intrinsic pathway. Upon attachment of P70 to the surface, the surface charge became more negative.

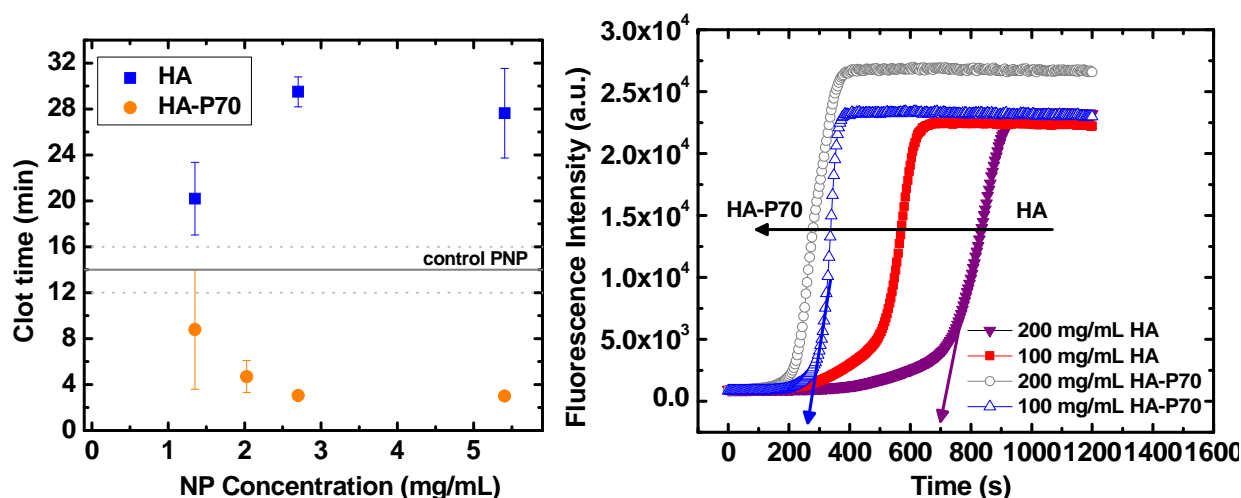


**Figure 20 – (Left) Attaching P70 to HA NPs creates a procoagulant from an anticoagulant scaffold. (Right) HA-P70 accelerates thrombin generation when compared to bare HA.**



**Year 02, Task 3 — Design and test particles that will function as candidate TSPs. SUBTASK 3.c Attach clotting triggering/enhancing agents to particles identified in task 3.a; also attach molecules that allow targeting/clustering of these particles in order to create candidate TSPs. Months 1-3.**

Among the issues in designing a viable TSP, limiting nanoparticle aggregation plays a key role. This issue becomes magnified due to the necessity of replacing ethanol with water in the nanoparticle solution to attach polyphosphate. The nanoparticles are usually centrifuged several times, discarding the supernatant and redispersing the pellet in water. Ideal particles will be sub-100nm in size with a polydispersity index below 0.1. One of the strategies studied to combat this problem was to use dialysis instead of centrifugation to remove the ethanol. Sub-100 nm silica nanoparticles were synthesized using the Stober method. After synthesis, one-half of the synthesis was dialyzed into water to attach polyphosphate, while the other remained in ethanol to attach APTES. The APTES-functionalized silica was then dialyzed in water before adding PEG to protect the surface. Through all stages of functionalization, the particles remained under 100 nm in size. Except for the APTES stage (~0.150 PDI), the PDI remained below 0.1. While dialysis succeeded in producing small monodisperse particles, the lengthy process and low recovery limits the effectiveness of dialysis.

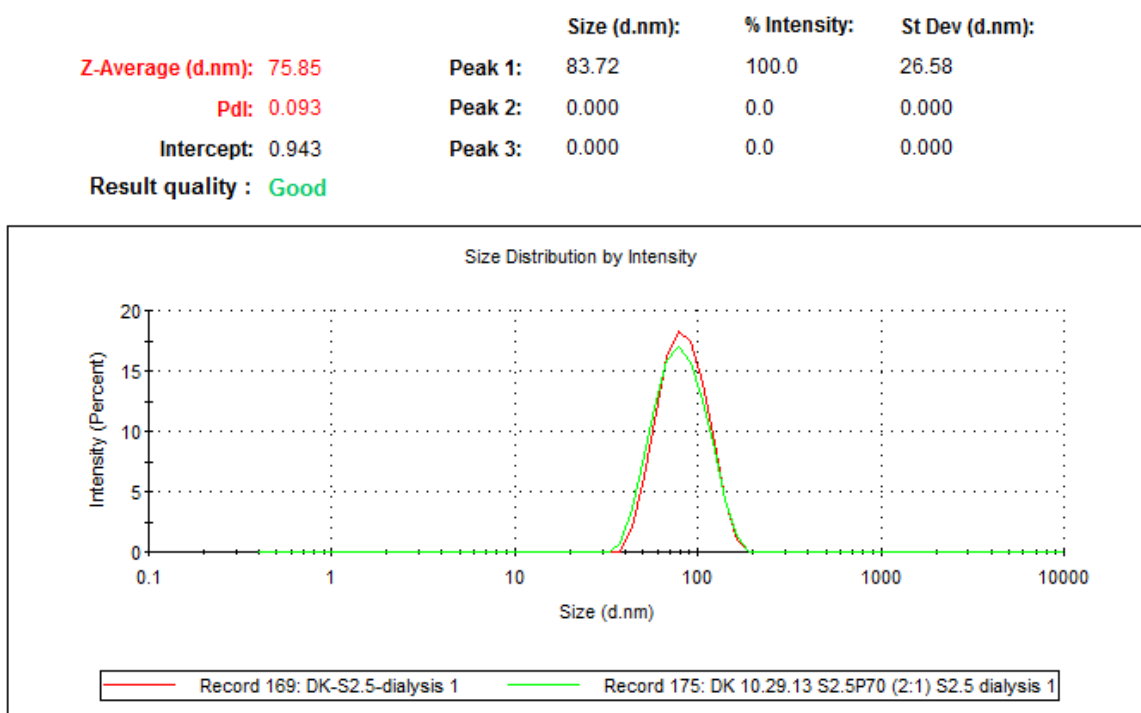


**Figure 21 – Bare silica nanoparticles (red) and P70 functionalized silica nanoparticles (green) after dialysis in water.**

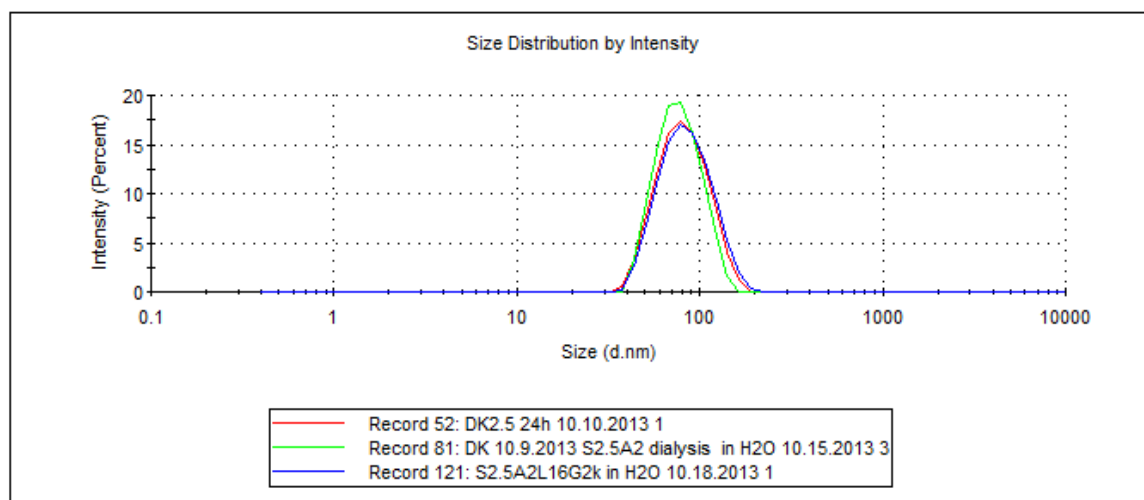


**Figure 22 – SNP (red), SNP+APTES (green), SNP+APTES+PEG (blue). Through the functionalization steps, the particle sizes remained under 100nm. However, SNP+APTES resulted in slightly elevated PDI.**

In addition to the Stober method, the reverse micelle method of silica particle synthesis was used to improve the uniformity and monodispersity of the particles. Scanning electron microscopy (SEM) characterization showed particles synthesized using reverse micelle method with a mean diameter of 44 nm and a standard deviation of 3 nm.

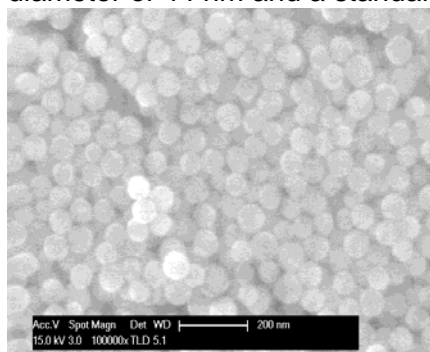


**Figure 23 - SEM characterization of silica nanoparticles prepared by the reverse micelle method. Particle size ranged from 37-50 nm with a mean of 44 nm and a standard deviation of 3 nm.**

Though the method gives added control over particle size, , the potential for undesired uptake of the silica nanoparticles into the lungs or other organs if the particles are too small, and the potential for unwanted obstructing small arterioles or capillaries if the particles are too large, were the main motivating factors for synthesizing particles of approximately 50 nm in size. Future efforts include further refinement of the synthesis process to better attain the desired mean particle size of 50 nm with less deviation, gram scale synthesis of the silica particles for subsequent functionalization with polyphosphate and associated linkers and protecting groups, characterization of the functionalized particles, and determination of the clotting effectiveness of the functionalized particles.

**Year 02, Task 3 — Design and test particles that will function as candidate TSPs. SUBTASK 3.c Attach clotting triggering/enhancing agents to particles identified in task 3.a; also attach molecules that allow targeting/clustering of these particles in order to create candidate TSPs. Months 1-3.**

One of the topics discussed at the Caltech meeting was the aggregation of bare SNP and SNP-P70 nanoparticles. At higher concentrations, the TSPs appear to aggregate in phospholipid solution. In the upcoming quarters, we intend to test the targeting/clustering of our TSPs in microfluidic devices with the Ismagilov group. If the particles aggregate when activated, it requires a lower general concentration to reach the local threshold at the wound site. We will use the results from assays run under flow conditions to tune our targeting strategies.

In addition to PEGylating particles for protection, we are developing a nanoparticle core covered by a polyphosphate “corona.” As short-chain polyphosphate is a poor initiator, the corona will allow the particle to rapidly accelerate coagulation in damaged vessels while minimizing impact in healthy vessels. Using a strategy developed in the Morrissey group, polyphosphate functionalized with the cross-linker 1-Ethyl-3-(3-dimethylaminopropyl)carbodiimide, EDC, binds to APTES.<sup>7</sup>

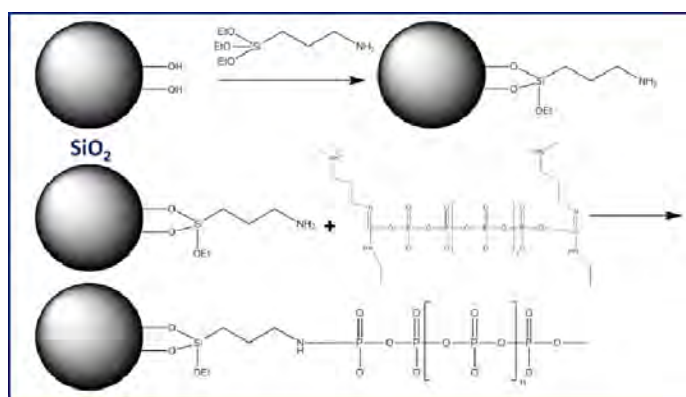


**Figure 24 - Mechanism for attaching polyP to SNP via APTES bridge. The polyP is first modified with EDC before addition to SNP-APTES.**

When tested using DLS, the APTES-functionalized particles exhibited a strongly positive charge. Upon addition of the EDC-functionalized P70, the particles once again held a negative charge. This suggests that the synthesis succeeded. However, the particles aggregated early on with the addition of APTES. Successful functionalization with EDC was difficult to verify via DLS and zeta measurements. To limit aggregation, we are looking at different linking methods that do not involve APTES.

<sup>7</sup> SH Choi, JN Collins, SA Smith, RL Davis-Harrison, CM Rienstra, and JH Morrissey. (2010). Phosphoramidate end labeling of inorganic polyphosphates: facile manipulation of polyphosphate for investigating and modulating its biological activities. *Biochemistry*, 49(45), 9935-41.

	Mean (mV)	Area (%)	St Dev (mV)
<b>Zeta Potential (mV): 23.9</b>	<b>Peak 1: 23.9</b>	<b>100.0</b>	<b>6.44</b>
<b>Zeta Deviation (mV): 6.44</b>	<b>Peak 2: 0.00</b>	<b>0.0</b>	<b>0.00</b>
<b>Conductivity (mS/cm): 0.0134</b>	<b>Peak 3: 0.00</b>	<b>0.0</b>	<b>0.00</b>
<b>Result quality : Good</b>			

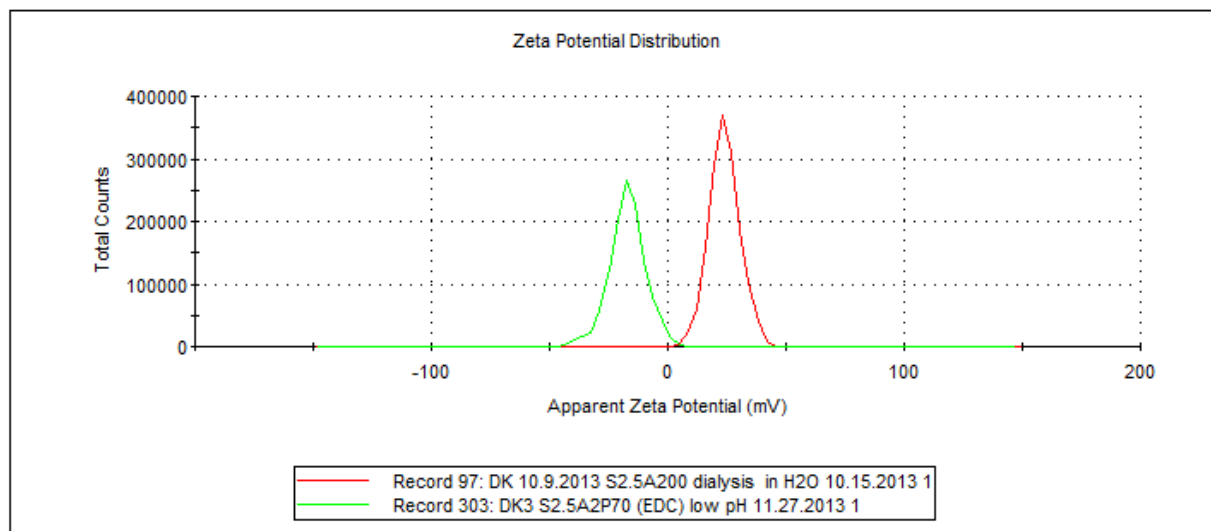


**Figure 25 - SNP-APTES (red) particles hold a positive charge. Upon addition of polyphosphate to the SNP-APTES (green), the charge becomes negative**

**Year 02, Task 3 — Design and test particles that will function as candidate TSPs. SUBTASK 3.d Quantify the procoagulant activities of the candidate TSPs created in task 3.c**

Previous work in the Stucky and Morrissey groups compared the clotting activity of SNP-P70 to lipidated tissue factor (LTF) – the body’s main response to vessel injury – under normal and traumatic conditions. The traumatic conditions are tied to coagulopathy – the fundamental breakdown of the clotting cascade and ensuing inability to form stable clots. Along with coagulopathy, hypothermia and acidosis form the “lethal triad.” All three states comprising the lethal triad are linked to increased mortality from traumatic injuries. While patients suffering internal hemorrhage may not exhibit characteristics of the lethal triad, TSPs that can counteract such dire conditions will help patients clot quicker and limit the adverse effects of internal blood loss. Hemodilution and hypothermia were the traumatic conditions studied in Q1.

Hemodilution was used to mimic the loss of factors as a result of exsanguination, consumption and fluid replacement. To create hemodilute plasma, normal PNP was mixed with Dulbecco’s Phosphate-Buffered Saline (DPBS). In all assays, 0.25 mg/ml SNP-P70 outperformed LTF at concentrations of 0.185 ng/ml, 0.5 ng/ml and 1 ng/ml. Most importantly, LTF was unable to initiate clotting or thrombin generation under 33 % PNP – 33 % PNP mixed with 67 % DPBS. Thus, we believe that the human body alone can no longer reach the coagulation threshold after losing 67 % of its procoagulant factors. Upon replacing LTF with SNP-P70 as the activating agent, thrombin generation and clot formation occurred rapidly. This suggests that the hemodilutional threshold for inducing coagulation with SNP-P70 is below 25 % of physiological concentration.

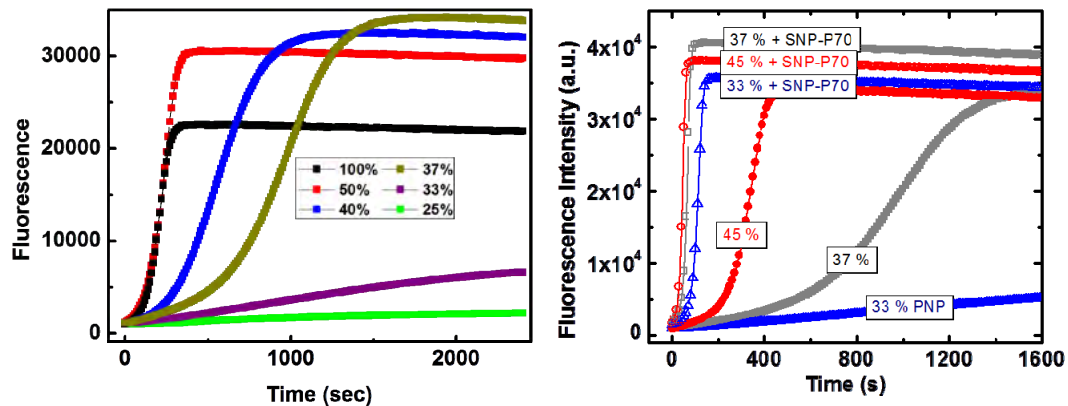


**Figure 26 – (Left) Diluted plasma with LTF. Below 33 % PNP, thrombin generation by LTF is null. (Right) SNP-P70 generates thrombin under severe hemodilution even when LTF cannot.**

Hypothermia, the second member of the lethal triad, occurs when the body temperature drops below 37 °C. The drop in temperature leads to a decreased kinetic rate of protein activation. As with the hemodilution assays, a hypothermia baseline was established using LTF. A major reduction in clot time and thrombin formation occurred when the plasma was chilled below 35°C. The decrease in clot time and thrombin generation was also seen when using SNP-P70. However, the decrease in clot time and activity due to hypothermia was again minimized by addition of SNP-P70 to hypothermic plasma.

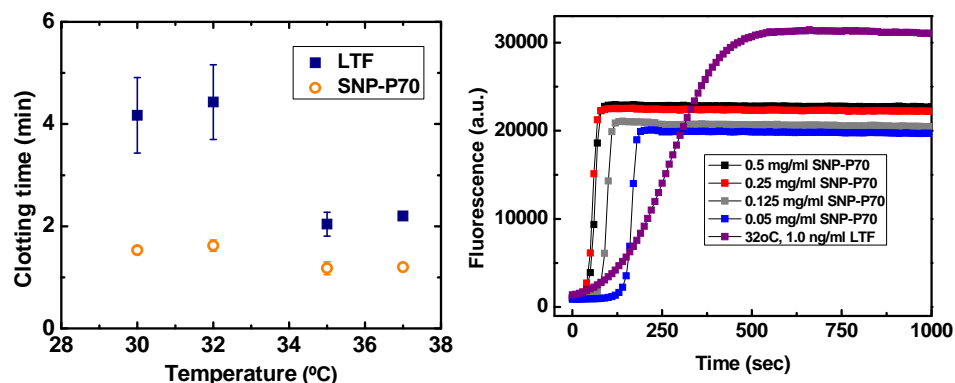


**Figure 27 – (Left) Clot time measured by TEG as a function of temperature of PNP with LTF or SNP-P70. SNP-P70 initiates clots more quickly under hypothermia conditions. (Right) At 32°C, SNP-P70 reaches maximum thrombin generation well before 1 ng/ml LTF.**

Of the lethal triad, acidosis causes the greatest problem to trauma patients. Normal blood has a pH of 7.4, which drops as a result of trauma. While sodium bicarbonate can return the blood's pH to a normal level, effects from acidosis continue to plague coagulopathic patients for roughly 24 hours.<sup>8</sup> Acidosis has been linked to decreased platelet count and FV activation. As this is the pathway by which polyP induces coagulation, we believe that the SNP-P70 will act as artificial platelets to add polyP to acidotic plasma or blood to achieve the desired threshold by increasing FVa concentration and clotting activity. We are currently refining our acidosis protocol to ensure reliable results. Lactic acid – produced in the muscles and released into the blood as a result of traumatic injury – is the current acidifying agent under consideration.

<sup>8</sup> Martini, W (2009). Coagulopathy by Hypothermia and Acidosis: Mechanisms of Thrombin Generation and Fibrinogen Availability. The Journal of trauma, 67(1), 202-209.

In testing the polyphosphate corona nanoparticles, we are looking for a Goldilocks solution. We have developed particles that are strong procoagulants, but will cause too many complications to be effective. Overly-protected particles that are too weak to improve clotting fail because they cannot prevent significant blood loss. By increasing the ratio of APTES to 200ul APTES per gram silica, we were able to increase clotting time in “healthy” plasma. This meant that the corona particles were not as successful at initiation clotting as particles with a more exposed silica surface.

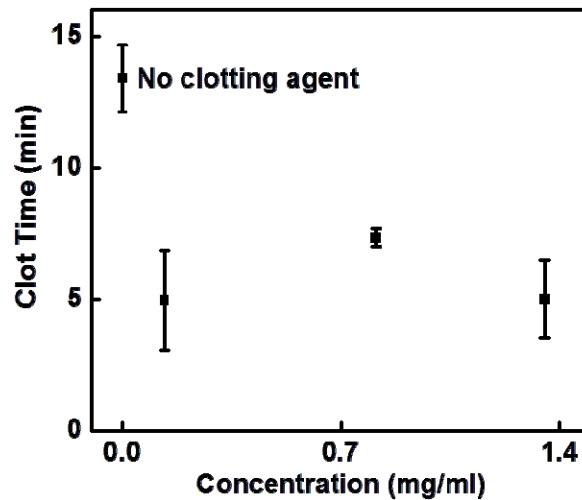


**Figure 28 - Polyphosphate corona particles have an increased clotting time above 5 min.**

In the presence of clotting, the polyphosphate corona should rapidly accelerate clotting to prevent blood loss. When lipidated tissue factor (LTF) was added to simulate an injury in our experiments, the particle and LTF combination reduced clotting by half compared with tissue factor alone. These results suggest that there is potential in delivering the polyphosphate without exposing the core. In the coming quarter, we aim to improve the synthesis to better cover the core and create a particle that is non-coagulating in healthy plasma while still accelerating coagulation in the presence of tissue factor. Among the ways we intend to test this is to replace the silica core with an inert compound such as calcium hydroxyapatite or *poly(lactic-co-glycolic) acid* (PLGA).

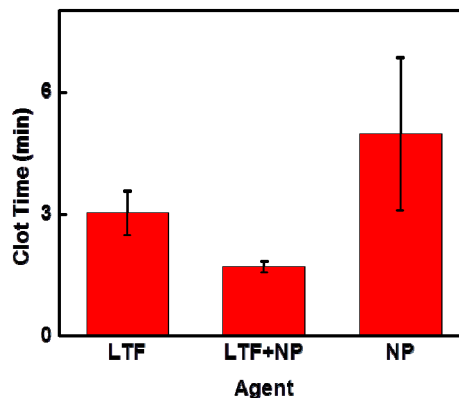


**Figure 29 - In the presence of tissue factor, the polyphosphate corona particles reduce clotting times in half.**

**Milestone #4** – Obtain candidate TSPs with high procoagulant activity when clustered, but with little to no procoagulant activity when finely dispersed in plasma/blood

We have conducted some thrombin-generation assays using a pelleted version of SNP-P70 under static conditions. These experiments showed a slightly lower clotting time compared to that of SNP-P70 in solution. However, these experiments favor nanoparticles in solution when run under static conditions. When attached to the well instead of in solution, the 100ul sample of plasma has less surface area to activate on a pelleted SNP-P70 than SNP-P70 in solution. This is the reason for the slightly elongated thrombin generation times. We are working to test the pelleted nanoparticles under flow to better estimate their clotting activity. Under flow, the clustering simulated by pelleting the SNP-P70 particles should reach the threshold easier than particles in solution which may never aggregate in a sufficient concentration to achieve coagulation. Only under flow conditions can we closely mimic *in vivo* conditions.

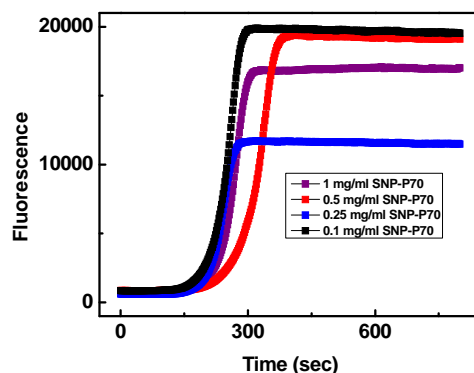


**Figure 30 - Clotting assay of pelleted SNP-P70. SNP-P70 was dissolved in ethanol and evaporated overnight to attach to the well surface prior to experiment.**

**Specific Aim #3** — Test the TSP system *in vitro* using human whole blood in microfluidic devices and *in vivo* using an animal model of incompressible hemorrhage, and use the results to establish a definitive predictive model for design of TSPs.

The Stucky, Morrissey and Ismagilov labs are currently working to develop protocols for testing the protected and unprotected SNP-P70 TSPs *in vitro* using microfluidic devices. We aim to begin testing the TSPs under flow conditions in the near future. Among the TSP attributes we will test for include activation under flow, clustering, thrombin generation and clot formation.

## KEY RESEARCH ACCOMPLISHMENTS

### Production of raw materials for conjugation to nanoparticles:

- Finished developing reproducible and scalable procedures for production of gram quantities of purified polyP of carefully defined size ranges, which is important in controlling the procoagulant activity of polyP

### Coupling chemistries for conjugation of polyP to nanoparticles:

- Defined optimal storage conditions for preserving phosphoramidate linkages to polyP
- Developed a robust method for coupling alcohols to polyP via ester linkages; used this to develop a novel chromogenic substrate for endo- and exopolyphosphatases (polyP degrading enzymes)
- Identified potential method for coupling carboxylates to polyP via mixed anhydride linkages

### Microfluidics:

- Developed microfluidic devices that now allow us to examine the clot-promoting activities of nanoparticles as a function of the local shear rate (to simulate blood flow in arteries, veins and capillaries, as desired).

### Development of polyP-based procoagulant nanoparticles:

- Identified conditions that permit formation of polyP-based nanoparticles based on nanoprecipitation, and determined that these particles are procoagulant
- Identified the contributions of plasma divalent metal ions on polyP solubility and nanoparticle formation; identified polyP nanoparticle growth kinetics
- Developed and characterized the properties of polyP-PLGA nanoparticles
- Developed a novel method for detecting and quantifying plasma clotting using a rheology-based “capillary pinch-off” method, and demonstrated its suitability for measuring plasma clotting times using very low-volume samples
- Optimized the production and use of SNP scaffolds for creating procoagulant polyP-carrying nanoparticles; made progress on optimal formulations to achieve desired level of procoagulant activity
- Evaluated the use of APTES-functionalized particles and PEG masking to create masked nanoparticles that could be unmasked at sites of injury
- Evaluated surface charge of nanoparticles as a means of controlling their ability to trigger the contact pathway of clotting relative to their ability to accelerate downstream clotting reactions.
- Achieved improvements in uniformity and monodispersity of nanoparticles
- Evaluated efficacy of candidate TSPs under simulated conditions of coagulopathy due to hemodilution and reduced core body temperature



## REPORTABLE OUTCOMES

- Gram quantities of purified polyP of carefully defined size ranges, facilitating nanoparticle synthesis
- Optimal storage conditions for preserving phosphoramidate linkages to polyP
- New coupling chemistries (ester and mixed anhydride linkages) for covalently attaching polyP to nanoparticles
- Novel chromogenic substrates for detecting polyP degrading enzymes
- Microfluidic devices that permit evaluating clot-promoting activities of nanoparticles at defined shear rates
- PolyP-PLGA nanoparticles
- Novel, rheology-based detection system for plasma clotting
- Optimized SNP scaffolds for procoagulant polyP-carrying nanoparticles
- Progress in evaluating PEG masking of procoagulant nanoparticles
- Progress in understanding performance of TSPs under simulated coagulopathy conditions
- PolyP-based nanoparticles based on nanoprecipitation; determined that polyP can be both the substrate and the triggering agent of the particle, which is biodegradable and biocompatible. With further modification, a “smart” particle system can be developed for targeting blood clotting (**Fig. 31**).

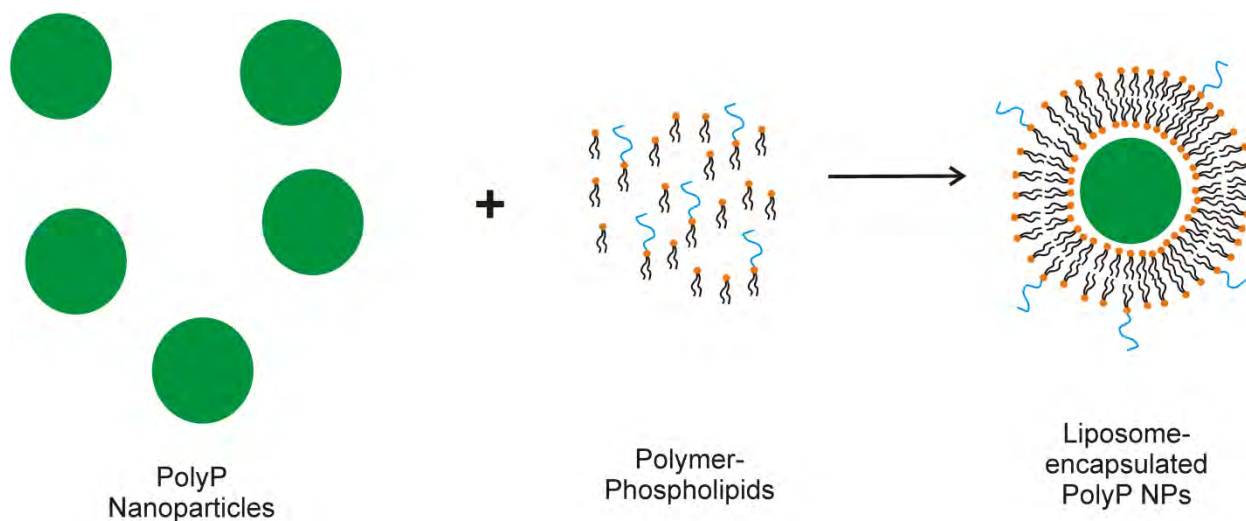


**Fig. 31.** Scheme for generating colloiddally stable, smart polyphosphate nanoparticles. Aqueous polyphosphate will first be precipitated in 5 mM  $\text{CaCl}_2$  solution buffered by 8 mM Tris-HCl at pH 7.4. It will subsequently be mixed with a mixture of phospholipid and polymer-phospholipid conjugates and extruded to generate liposome-encapsulated polyP NPs that exhibit long half-life and do not agglomerate.

### Recent Publications:

- Patent application: UC Case 2013-559 titled “POLYPHOSPHATE-FUNCTIONALIZED INORGANIC NANOPARTICLES AS HEMOSTATIC COMPOSITIONS AND METHODS OF USE,” submitted March 8, 2013.

## CONCLUSION

Specific Aim #1 of the statement of work calls for using theory and experiments to identify the most promising mechanisms to switch from below- to above-threshold conditions to initiate local clotting. The Ismagilov lab was delayed in pursuing this aim owing to its relocation to Caltech but is now working actively on this topic in a close collaboration with Dr. Christian Kastrup.

Specific Aim #2 of the statement of work calls for the design of a threshold-switchable particle system with a paired particle and trigger to target internal hemorrhage. The proposal calls for us to identify nanoparticles as scaffolds and to test procedures for attaching procoagulant materials to the nanoparticles. The Morrissey lab has previously developed high-yield, scalable methods for carefully size-fractionating polyP and this has been matured so that sufficient quantities can now be utilized in producing nanoparticles by the Stucky and Liu labs. The Morrissey lab has also developed novel coupling chemistries for polyP and provided better understanding of the stability of the polyP adducts. It has also developed tools to assist in working toward stabilizing polyP-based nanoparticles when they will be circulating in the blood.

The Stucky and Liu groups have continued to make progress on novel nanoparticle formulations and have continued progress using previously-reported nanoparticle types, along with developing and testing new formulations of procoagulant nanoparticles, including PEG-masked nanoparticles as well as self-assembling nanoaggregated particles based on polyP. This research has helped to define the parameters that modulate the procoagulant activities of the various candidate nanoparticles formulations. In the near future, work in the Ismagilov and Kastrup groups will focus on determining the threshold conditions for these nanoparticles and define how they function under flow.

In the remaining time period, the Ismagilov and Kastrup groups will use numerical simulations and microfluidics measurements to refine the parameters for TSP-induced blood clotting and identify threshold conditions. The Liu and Stucky groups will continue to develop, evaluate and mature a variety of polyP-based nanoparticle formulations that show promise as TSPs, which will be tested by the Ismagilov, Kastrup and Morrissey groups. The goal remains to identify several new TSP systems with the potential to treat internal hemorrhage.

*“So-What Section”:* The final goal of these studies is to develop advanced nanoparticles engineered to stop internal (incompressible) hemorrhage. If we are successful, we will create regulated clotting activators that can circulate in the blood at below the threshold necessary to trigger clotting, and therefore not cause unwanted thrombosis. However, the nanoparticles will ultimately be engineered to accumulate at sites of internal injury/bleeding, where their local concentration will greatly exceed the threshold for clotting activation, thereby restoring hemostasis. This has the potential to treat otherwise untreatable, life-threatening internal bleeding associated with trauma.

## REFERENCES

- [1] Smith SA, Mutch NJ, Baskar D, Rohloff P, Docampo R, Morrissey JH. Polyphosphate modulates blood coagulation and fibrinolysis. *Proc Natl Acad Sci U S A*. 2006;103:903-8.
- [2] Morrissey JH, Choi SH, Smith SA. Polyphosphate: an ancient molecule that links platelets, coagulation, and inflammation. *Blood*. 2012;119:5972-9.
- [3] Muller F, Mutch NJ, Schenk WA, Smith SA, Esterl L, Spronk HM, et al. Platelet Polyphosphates Are Proinflammatory and Procoagulant Mediators In Vivo. *Cell*. 2009;139:1143-56.
- [4] Shoffstall AJ, Atkins KT, Groynom RE, Varley ME, Everhart LM, Lashof-Sullivan MM, et al. Intravenous hemostatic nanoparticles increase survival following blunt trauma injury. *Biomacromolecules*. 2012;13:3850-7.
- [5] Choi SH, Collins JN, Smith SA, Davis-Harrison RL, Rienstra CM, Morrissey JH. Phosphoramidate end labeling of inorganic polyphosphates: facile manipulation of polyphosphate for investigating and modulating its biological activities. *Biochemistry*. 2010;49:9935-41.
- [6] Müller F, Mutch NJ, Schenk WA, Smith SA, Esterl L, Spronk HM, et al. Platelet polyphosphates are proinflammatory and procoagulant mediators in vivo. *Cell*. 2009;139:1143-56.